J.G. Zondervan

Department of Hydraulics and Catchment Hydrology, Agricultural University, Wageningen

Modelling urban run-off; a quasilinear approach

Centre for Agricultural Publishing and Documentation

Wageningen – 1978

ISBN 90 220 0665 4

The author graduated on 12 May 1978 as Doctor in de Landbouwwetenschappen at the Agricultural University, Wageningen, the Netherlands, on a thesis with the same title.

Abstract

Zondervan, J.G. (1978) Modelling urban run-off – a quasilinear approach. Agric. Res. Rep. (Versl. landbouwk. Onderz.) 874, ISBN 90 220 0665 4, (vi) + 68 p., 48 figs, 9 tables, 46 refs, 3 App., Eng. and Dutch summaries.
Also: Doctoral thesis Wageningen.

The non-linear behaviour of catchments, as ascertained by various investigators, is discussed. Blackbox analysis with Laguerre functions shows non-linear behaviour for a small urban catchment area. Some approaches to non-linear systems for rainfall and run-off are considered. Two quasilinear methods are compared with a theoretical model for their application. Results from an application of the most promising method on an urban catchment area confirm the feasibility of this method. Six conceptual models are compared and an application of the quasilinear method is given with a conceptual model. A satisfactory treatment of losses forms a major problem in modelling urban rainfall and run-off. Hence a chapter is devoted to transformation of rainfall into sewer inflow and concurrent losses. The use of critical sequences of rainfall for modelling is discussed. Evidence suggesting the maximum time interval between samples is given.

Free descriptors: urban hydrology, catchment area, sewer run-off, infiltration losses, critical sequences of rainfall.

Contents

Errata to Zonĝervan, J.G., 1978. Modelling urban run-off - a quasilinear approach. Agric. Res. Rep. 874
Also: Doctoral thesis Wageningen

Page	Line	Remarks
Preface	11	'assistence' should be 'assistance'
1	38	'sample' should be 'samples'
2	35	'Lelystad 1 ...(1977).' should be 'Lelystad 1, the interval between samples has to be about 2 minutes. Only for a catchment'
3	Table 1	'Hamilton Hiils 5' should be 'Hamilton Hills 5'
6	36	'ten' should be 'eleven'
7	25	'run-off rate' should be 'ultimate run-off rate'
	45	'1.8' should be '2.4'
20	7	'complications.' should be 'complications,'
	8	'rater' should be 'rather'
	36	'parameter' should be 'parameter,'
24	11	'soil' should be 'soil.'
25	18+19	'These high ... rainfall' should be 'These high 'losses' can be ascribed to strong variability of rainfall, resulting in a poor representation of rainfall'
34	3	'ν' should be 'ν'
	7	'upstram' should be 'upstream'
37	Table 5	'+0.26' should be '-0.26'
		'+0.22' should be '-0.22'
45	39	'waarover' should be 'waarvan'
59	14	'Table A3.2' should be 'Table A3.2.'

1 Introduction

In the last decennia, urban growth has been rapid in many parts of the world. The concurrent problems of flash floods and deterioration of water quality have increased awareness of the need for integrated regional water management in such urban areas.

The aim of modelling is to provide tools for water management, in which the various interests and their interactions are taken into account (e.g. McPherson, 1974). Although such water management ultimately requires models for both water quantity and water quality, this study is restricted to a number of quantitative aspects of modelling.

McPherson (1976) points out that 'mathematical model development for sewered system applications has seemingly already greatly outpaced the data base for model verification'.

In this study, analysis of existing data indeed showed that their accuracy is often inadequate for developing models. Analysis of a number of short-term records of rainfall and run-off showed that often one raingauge does not sample the time distribution of areal rainfall with sufficient accuracy, especially for heavy local thunder storms which are the source of critical loads on the sewer system. For instance, for an airport with a catchment area of only 0.3 km^2, with all the surface developed, total run-off could be 1.3 times the recorded rainfall. Another difficulty that sometimes prevents use of data is too long a sample interval. A third difficulty in modelling rainfall and sewer run-off from urban catchment areas is that even if one has reliable data on rainfall and run-off, data on antecedent rainfall are often lacking. That information is however essential for research.

Because of such difficulties, only the analysed data of one small urban catchment area were found that suited detailed research. The size of the catchment area, a residential quarter in the United States town of Gray Haven, Maryland, is 94 000 m^2.

Non-linear behaviour as found for the Gray Haven catchment area could also be demonstrated for a much larger urban catchment area in the town of Enschede in the Netherlands. The data of this catchment, however, which were used for a blackbox analysis (van der Kloet et al., 1977), could not be used for detailed research, because there also the size of the catchment area, 1.4 km^2, was too large to justify use of rainfall data from one raingauge only. Because of the non-linear behaviour encountered in these urban catchment areas, this study concentrates on recent approaches to non-linear hydrological systems.

Losses by ponding and infiltration are so important in modelling, that much effort was given to developing equipment for measuring such losses. Experiments with the equipment in urban study areas where the rainfall and run-off is measured, can yield valuable complementary information.

Use of models for the transformation of rainfall into sewer run-off requires sequences of rainfall with a short time interval. For some sizes of catchment area, evidence on the permissible maximum interval between sample is given.

2 Rainfall data to compute run-off from small urban catchment areas

This chapter considers only point rainfall. To allow the computation of run-off hydrographs caused by extreme rainfall from urban catchment areas, both critical sequences of rainfall and a model for the transformation of rainfall into run-off are needed.

For computations of extreme run-off often the simplifying assumption is made that rate of rainfall is constant for a certain time T. Rate of rainfall can then be obtained from intensity–duration–frequency curves. An example of this procedure is the well known 'rational method', which Watkins (1963) reports to have been used in Ireland by Mulvaney as early as 1851. Ardis et al. (1969) by an investigation into the storm drainage practices of thirty-two cities in the United States, found that at that time practically every city still used this method for design purposes. McPherson (1969) clearly demonstrated the crudeness and limitations of this method.

An example for the Netherlands in which the assumption of a constant rate of rainfall is involved is the use of the 'dots graphic of Kuipers'. This graphic gives for the period 1938-1948, for all events with more than 4 mm precipitation at De Bilt, the relation between duration of rainfall and amount. The graphic of Kuipers is a frequently used tool for estimation of frequencies of spills from sewer systems in the Netherlands (Koninklijk Instituut van Ingenieurs, 1972; Schenkeveld, 1976). Here again the assumption of constant rainfall during a time T may lead to erroneous results. In its report of 1972 the Koninklijk Instituut van Ingenieurs (Royal Institute of Technical Graduates) shows that use of the graphic of Kuipers underestimates the frequency of spills from sewer systems. The assumption of constant rate of rainfall within T gives rise to bigger errors as the response time of the considered system is smaller in comparison with T.

Urban systems for rainfall and run-off often have such short response times that, if hydrographs must be computed from rainfall data, it is necessary to have data with a small interval between samples. To illustrate this, in Table 1 the lag times for a number of small sewered urban catchment areas and inlet areas in the United States (Shaake jr. et al., 1967) and the Netherlands are given. The Dutch inlet areas Pomona, Bennekom and De Nieuwlanden are described in Chapter 3. The lag times of the Dutch catchment areas Lelystad 1, Lelystad 2 and Varviksingel were taken from van der Kloet et al. (1977). Lelystad 1 and 2 are a small residential quarter and a parking place, respectively, in the town of Lelystad. Varviksingel is a sewer district in the town of Enschede.

By rule of thumb that the sample interval must not exceed a quarter of the lag time of the catchment area, a sample interval of about 15 s would be appropriate for small inlet areas like Pomona and Bennekom. For small residential quarters like Gray Haven and Lelystad 1, Lelystad 2 and Varviksingel were taken from van der Kloet et al. (1977). area like Varviksingel, with an area of 1.4 km^2 would a sample interval of 5 minutes be sufficiently small.

In the Netherlands, statistical properties of rainfall are published by the KNMI (Royal

Table 1. Lag times for a number of urban catchment areas in the U.S.A. and in the Netherlands.

Catchment area	Area (10^3 m^2)	Imperviousness (%)	Average lag time
United States of America[1]			
Gray Haven	94.3	52	8 min 30 s
Hamilton Hills 2	3.9	20	8 min 42 s
Hamilton Hills 3	7.4	36	7 min 24 s
Hamilton Hills 4	0.9	96	4 min 54 s
Hamilton Hills 5	6.9	32	4 min 48 s
Midwood 5	5.2	56	3 min 6 s
Montebello 2	6.1	9	8 min
Montebello 3	1.8	57	4 min
Montebello 4	2.2	65	3 min 18 s
Montebello 5	2.1	66	3 min 42 s
Newark 9	2.6	100	3 min 24 s
Newark 12	3.9	100	4 min 54 s
Northwood	191.8	68	6 min 30 s
South Parking Lot 1	1.6	100	4 min 42 s
South Parking Lot 2	1.9	100	6 min 54 s
Swansea	190.6	44	4 min 48 s
Uplands	121.8	52	7 min 24 s
Walker Avenue	620.8	33	11 min 30 s
Yorkwood	42.1	41	4 min 42 s
Netherlands			
Pomona	0.15	100	1 min 36 s – 2 min 18 s
Bennekom	0.16	100	1 min – 2 min 5 s
De Nieuwlanden	0.43	100	3 min 3 s – 4 min
Lelystad 1	20.0	44	9 min – 11 min
Lelystad 2	7.1	97	5 min – 7 min
Varviksingel	1400.0	estim. 24	32 min – 40 min

1. From Schaake et al. (1967).

Netherlands Meteorological Institute). The shortest time interval for which statistical information can be obtained is 5 minutes (KNMI, 1968). This information on 5-minutes rainfall is based on charts of a self-recording raingauge, covering a period of 12 years. Hence rainfall records with an appropriate sample interval are available in the Netherlands for urban catchment areas larger than about a square kilometre. Because a record length of 12 years is not very long for extreme rainfall events, one could suggest the use of a model to simulate rainfall sequences. Such a model could be calibrated with the record of 5-minutes data of the KNMI.

Cole & Sherriff (1972) reviewed stochastic models for the simulation of rainfall over short time intervals. Only in two studies mentioned there was a time interval less than one hour used. Both studies, by Grace & Eagleson (1966) and Raudkivi & Lawgun (1970) used intervals of 10 min. The model of Grace & Eagleson was constructed to simulate critical sequences of rainfall data for small catchment areas in the northern part of the

United States and in Canada. Since critical sequences of rainfall for such catchment areas would be sudden heavy rain, which occurs typically in summer thunder storms, only summer data were analysed. In their analysis, they distinguished three types of storms.

Raudkivi & Lawgun (1970), who developed their model for the Auckland area in New Zealand, constructed a simulation model in which all types of rainfall were lumped. They dealt with the seasonality of the rainfall process by calibrating their model parameters for each month of the year.

In the Netherlands, many types of rain occur, for instance showers, cold fronts, warm fronts, frontal and non-frontal low pressure centres, and occluded fronts. As lumping of different types of rainfall is doubtfully justifiable and because also in the Netherlands critical rainfall sequences for small urban areas will be produced by short heavy summer showers, the approach of Grace & Eagleson must be preferred if it is decided to use a simulation model.

Yperlaan (1977) found evidence of an increase in precipitation near Rotterdam. To investigate the urban influence for different weather types, he selected precipitation days from 1958 up to 1970 according to season, wind direction and precipitation type. He found that frontal rains and rains in low pressure systems seem to give positive moderate differences, whereas for some showers very high increases seemed to result from urban influence.

These considerations lead to the following recommendations:

– As transformation of rainfall into sewer inflow for common Dutch road drainage is so fast that it can be neglected in modelling run-off from urban catchment areas, gathering rainfall data with a time interval of 15 s seems–ignoring technical difficulties–not necessary for modelling purposes. Whether a sample interval of 15 s is desirable for other purposes, as in the planning of number of inlets per area, will not be treated here.

– For modelling run-off from small urban catchment areas (5×10^3 to 200×10^3 m^2) a sample interval of one or two minutes is required. Because such 'urban drainage units' are appropriate for modelling purposes, creation of rainfall records with a one-minute interval is recommended. As short heavy summer showers are of special interest, the data must be reduced substantially at the site of the raingauge. As heavy summer showers have a local character, it is recommended to measure at more than one station with a one-minute interval, to obtain more quickly a number of critical rainfall events.

– Information on antecedent rainfall is important for modelling urban run-off (Chap. 3). This information, however, can be obtained from rainfall data with a much longer sample interval.

– The evidence of urban influence on precipitation as found by Yperlaan (1977) should be investigated especially for heavy summer showers.

– Since differences in types of rainfall, local influences on showers (urban, coastal) and periodicities in occurence of showers (thunder storms mostly occur during the second half of the day), the use of simulation models for short-term rainfall seems questionable. If it is decided to use such a model, it seems appropriate to confine simulation to summer showers.

– Finally, if one uses intensity–duration–frequency curves to obtain critical storms for computations of extreme run-off, one can introduce storm profiles instead of assuming constant rainfall. In this manner, Tholin & Kiefer (1960) determined a critical storm for sewer design in Chicago. They based their storm profile on the analysis of some measured storm profiles. For an extensive treatment on storm profiles, see the British Flood Studies Report, Vol. 2 (National Environment Research Council, 1975).

3 Transformation of rainfall into sewer inflow and concurrent losses

In the Netherlands (relatively flat regions and moderate rainfall rates) sewer run-off usually originates from rainfall on roofs and pavements only. Therefore it is common practice in Dutch sewer design to neglect run-off from pervious areas. On the other hand, losses that occur on the developed surfaces are also neglected.

Transformation of rainfall into sewer run-off can be represented by a transformation of rainfall into sewer inflow, followed by a transformation to sewer outflow in the sewer system itself. Although losses can take place during both transformations, it can be assumed that losses occur mainly before water enters the system of sewers, if the sewer system is in good condition.

In the town of Wageningen, two flat roofs of buildings of the University, each with a surface of about 1000 m^2, are being studied. This study, which is still running, will give information about the effect of the roof-covering (very fine pebbles, 3-4 mm diam., and coarse pebbles, 1-5 cm diam.) on the rainfall–run-off relation of flat roofs. On a part of one of these roofs at 'De Nieuwlanden', experiments were carried out with a rainfall simulator (Fig. 1) for a pioneer study. Details about the rainfall simulator and measuring equipment, and the detailed results of this study are given in Zondervan & Dommerholt (1975). A sketch of the roof and drains is given in Figure 2. The surface of the roof is tarred with a layer of 5 mm of the fine pebbles on top.

In this study the 'lag-and-route model' (a time shift + a linear reservoir) proved to be an adequate model for this inlet area (for a further description of this model see the first section of Chapter 6 on conceptual models). The lag time of the linear reservoir k was derived from recession curves (Fig. 3). These recession curves were obtained by simulating rainfall with an intensity of about 70 mm/h till equilibrium was reached, whereafter the rainfall was stopped and the run-off measured. If the lag-and-route model is a good one for the transformation of rainfall into run-off, the recession curve must yield a straight line on semi-log paper. This was approximately true except for very low flows (run-off $<$ 1.5 1/s $\approxeq$ 13 mm/h). From the slope of the recession curve a value of 2.5 min was derived for the lag time of the reservoir. The time shift τ was, as a first approximation, assumed to equal the average time of travel in the drains.

Another way of estimating the parameters of a model is to optimize them according to least sum of squared differences (LS) between measured and calculated run-off for a certain rainfall–run-off event. In this way, the parameters of a number of conceptual models, among which the lag-and-route model and the three-parameter model: convective diffusion, upstream inflow + time shift were optimized for a simulated shower on De Nieuwlanden. To eliminate the effect of the observed non-linear behaviour during the first minutes of rainfall, the first ten minutes of the shower were excluded from the LS.

For both models, the measured and optimized run-off hydrographs are given in Figures 4 and 5. For both, a value of 1 min was found for the time shift τ, which confirmed

the assumption in which τ was equated with the average time of travel in the drains.

The same shower was used to evaluate the performance of the lag-and-route model using the lag time of the reservoir as found with the recession curve (Fig. 6). The run-off simulation was satisfactory. The deviations between measured and simulated run-off during the first minutes of rainfall and in the tail of the run-off hydrograph are due to non-linearities, which are rather pronounced at low flows (Chap. 4).

No results of systematic investigations on the transformation of rainfall into sewer inflow and concurrent losses have been published in the Netherlands. Besides investigations on roof inlet areas, experimental equipment was developed to allow the study of paved inlet areas. With this mobile equipment, controlled flows were taken from fire hydrants and with a rainfall simulator this water was sprinkled on pavements. The resulting inflow into the sewer system was measured (Zondervan & Dommerholt, 1976; Dommerholt & Zondervan, 1977). Two typically constructed roads, a parking place paved with concrete stones at 'Pomona' in the town of Wageningen and an asphalt road with a tiled footpath on either side in the village of Bennekom were investigated (Fig. 7 and 8). Figure 9 is a map of two inlet areas at Pomona. A description of some experiments on the inlet area P III + P IV will be given to demonstrate the course of events. The inlet area was divided into two equal parts, because the rainfall simulator could not cover the whole surface.

To estimate the initial losses for wetting the surface and filling depressions, a constant rainfall rate of 72 mm/h was simulated as first and last experiment. The first experiment was started with a completely dry road surface. The shift between the rising limbs of the two run-off curves yielded a value for the initial loss (Fig. 10).

After some minutes of rainfall, run-off rate becomes almost constant. The difference between rainfall rate and run-off rate yields the infiltration rate that corresponds with the moisture condition at the moment. The figure shows that during the experiments between the first and last experiment, the infiltration rate decreased considerably.

In the laboratory, the infiltration rate of the concrete paving stones was determined as 0.5 mm in the first 15 minutes. After 15 minutes, infiltration almost ceased. Thus Figure 10 suggests that the observed infiltration mainly occurred through the joints between the concrete stones.

The lag-and-route model, which proved to be a succesful model for De Nieuwlanden was also tried out for these paved inlet areas. Figure 11 shows how the lag time k of the reservoir was estimated from recession curves for P III and P IV. Figure 12 shows simulated and measured run-off hydrographs from a composite shower for P III and P IV, using the parameters found in Figure 11. In the simulation, lag was not yet introduced. Figure 12 shows that by introducing a time shift of 30 s simulation is satisfactory. Figure 13 is a map of the experimental site at Bennekom. After estimating the lag time k from recession curves, the lag-and-route model was tried out as at Pomona. Figure 14 shows simulated and measured run-off hydrographs for the composite shower for B II. Here introduction of a time lag would hardly improve the result.

In the study of the inlet areas at Pomona and Bennekom, the lag-and-route model again proved adequate to describe the transformation from net rainfall into sewer inflow.

For the surface with paving stones at Pomona, the infiltration rate was between 7 and 27 mm/h. The initial loss varied between 0.5 and 1.8 mm. As the experiments were after

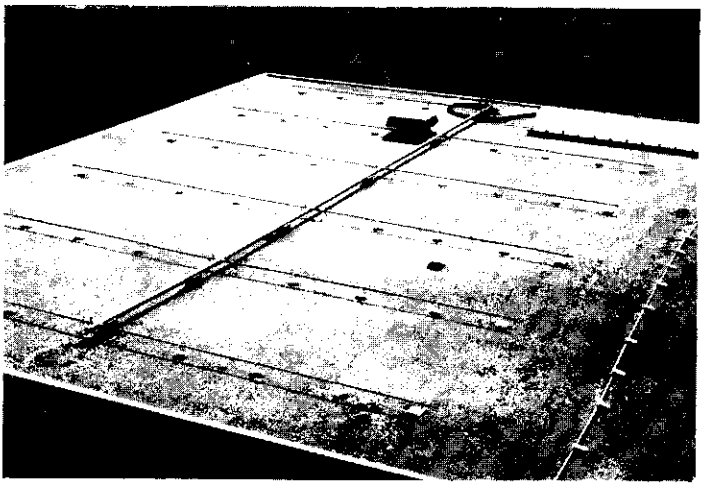

A

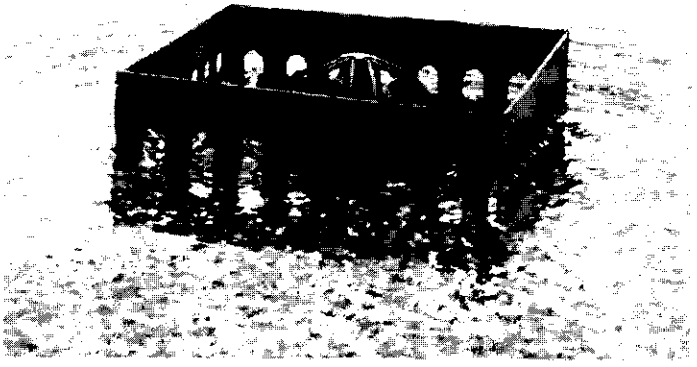

B

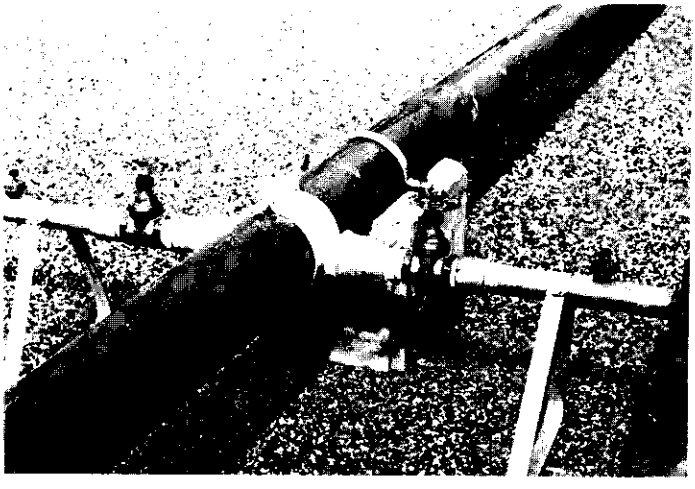

C

D

E

Fig. 1. Experiments on the roof of De Nieuwlanden. A. General layout, B. Drain inlet. C. Part of water supply and a sprinkler pipe. D. Sprinkler installation in action. E. Detail of D.

a long dry period, one would expect that on the average lower values for the infiltration rate will prevail. The described experiments however demonstrated that losses during the transformation of rainfall into sewer inflow can be high. More experiments at different sites are needed in order to evaluate the effect of previous rain on initial losses and on infiltration rate. Information on losses in urban catchment areas can also be obtained from rainfall–run-off studies on small well-gauged catchment areas. But to obtain information about losses on paved areas, the rainfall simulator method has some advantages:

– In catchment studies, errors in the rainfall data and leakage from the sewer system may disturb the results.

– With the mobile equipment, little time is needed to estimate losses at many sites and with various rainfall rates and initial moisture conditions.

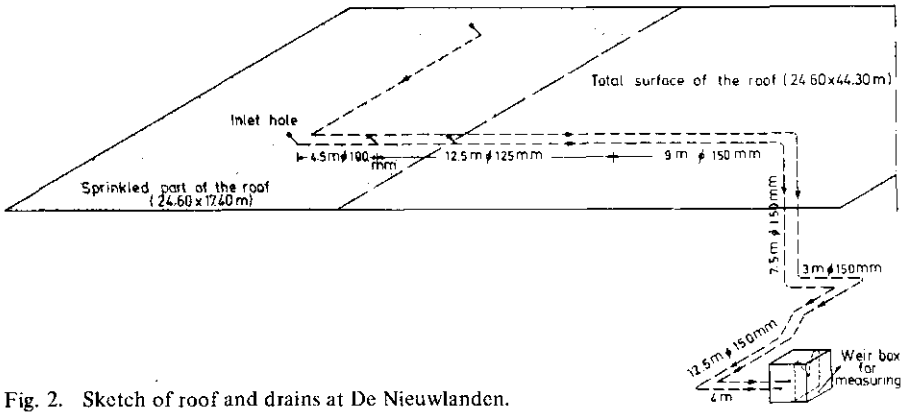

Fig. 2. Sketch of roof and drains at De Nieuwlanden.

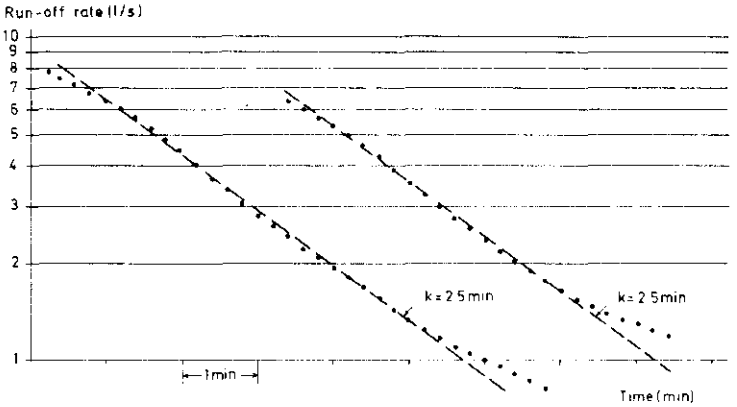

Fig. 3. Recession curves from experiments at De Nieuwlanden. k is parameter of the linear reservoir model.

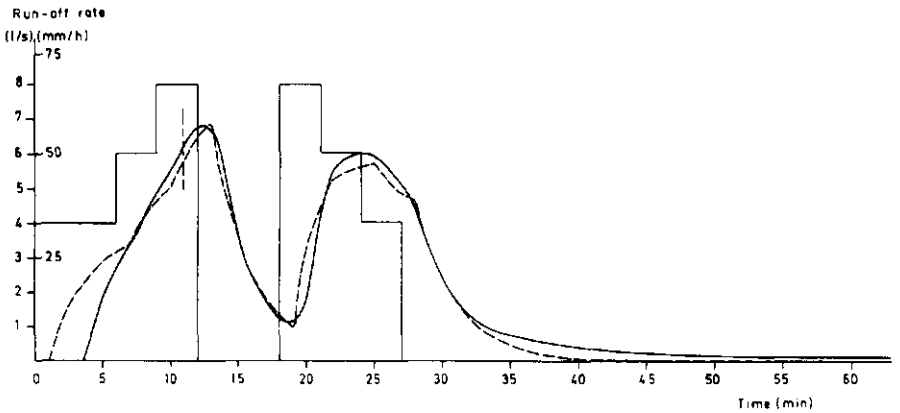

Fig. 4. Run-off simulation with the lag-and route model. The parameters were optimized for this storm according the least sum of squared differences (LS). Data from De Nieuwlanden experiments. ⎍rainfall, — observed run-off, – – – simulated run-off. Parameters: k = 3.1 min, τ = 1.0 min. LS: 8.22 l^2/s^2 (t = 11-63 min).

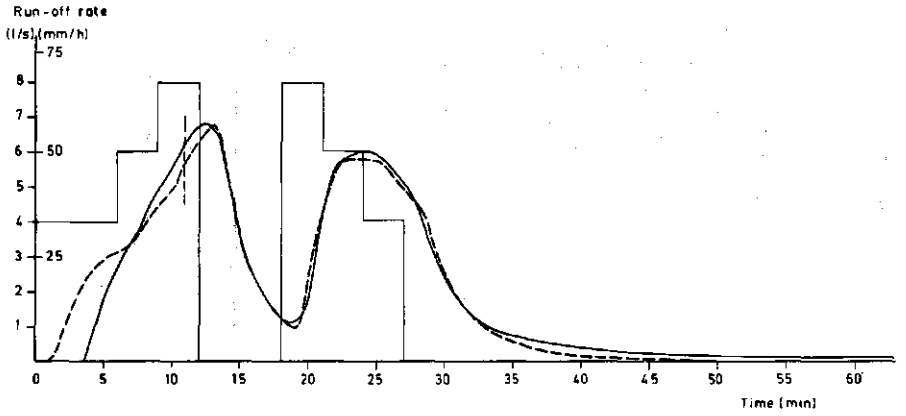

Fig. 5. Run-off simulation with the model convective diffusion, upstream inflow + a time shift. The parameters were optimized for this storm according to the least sum of squared differences (LS). Data from De Nieuwlanden experiments. ⎍ rainfall, — observed run-off, – – – simulated run-off. Parameters: $H = 0.80$, $I = 4$ min 27 s, $\tau = 1.0$ min. LS: 4.40 l^2/s^2 (t = 11-63 min).

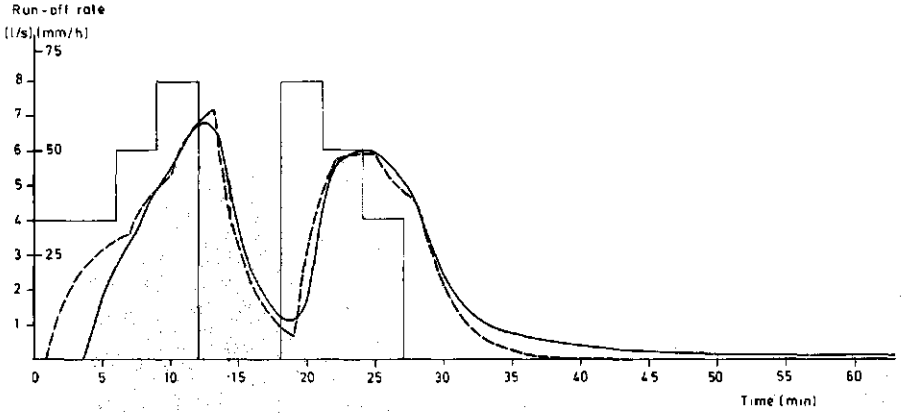

Fig. 6. Run-off simulation with the lag-and-route model. The lag time was obtained from the recession curves in Figure 3. ⎍ rainfall, — observed run-off, – – – simulated run-off. Parameters: $k = 2.5$ min, $\tau = 1.0$ min. LS: 12.91 l^2/s^2 (t = 11-63 min).

– In catchment studies, information on integrated losses is obtained and (as demonstrated later) the distribution of losses in time can only be guessed.

Catchment studies offer the opportunity to study the simultaneous behaviour of hydrological variables in the chosen area. One can study losses on the impervious surface, transformation of rainfall onto this surface into sewer run-off, conditions under which pervious surfaces may contribute to run-off and fluctuations in watertable.

Lack of information about losses as a function of time is one of the major problems in trying to model the transformation of rainfall into sewer run-off. As the processes that

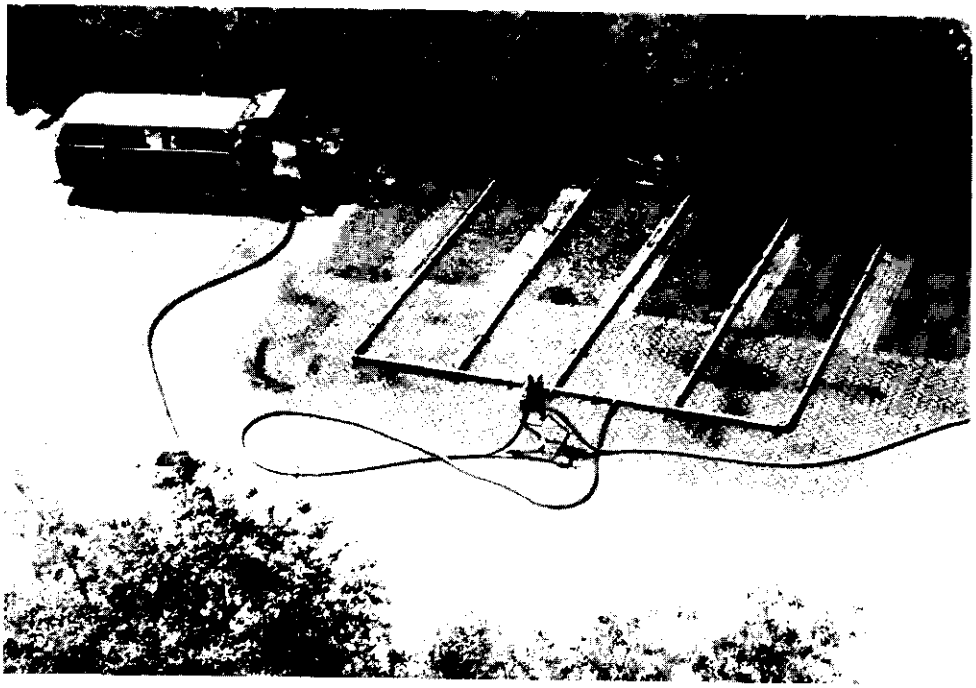

Fig. 7. Parking place at Pomona.

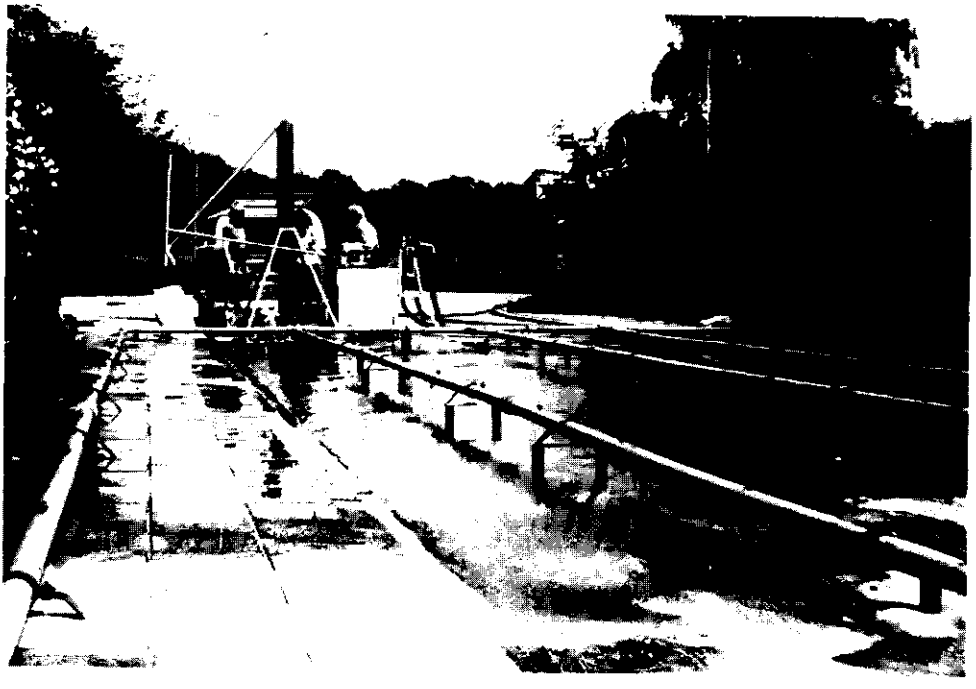

Fig. 8. Road at Bennekom.

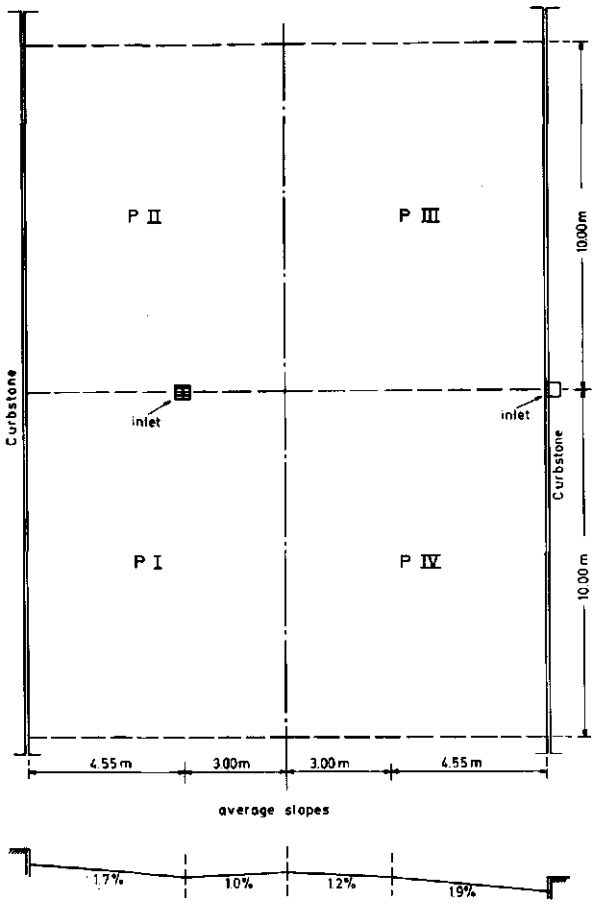

Fig. 9. Plan of the experimental site at Pomona.

determine the losses are complicated, the best thing that one can do is to try to describe the losses with a simple model. Well-known examples of such models are:

– A. Initial loss. Previous precipitation, by filling depressions and wetting the surfaces, quickens the response of a catchment area.

– B. The Φ index. Here a constant absolute loss rate is assumed during the whole period of rainfall excess.

– C. Proportion assumed lost.

– D. The combination A+B or A+C.

For an extensive treatment of the distribution of losses, the reader is referred to the British Flood Studies Report, Vol. 2 (Natural Environment Research Council, 1975).

It is possible to select between the Φ index and the proportional model for a certain catchment area, if records of rainfall and run-off are available. This can be achieved on

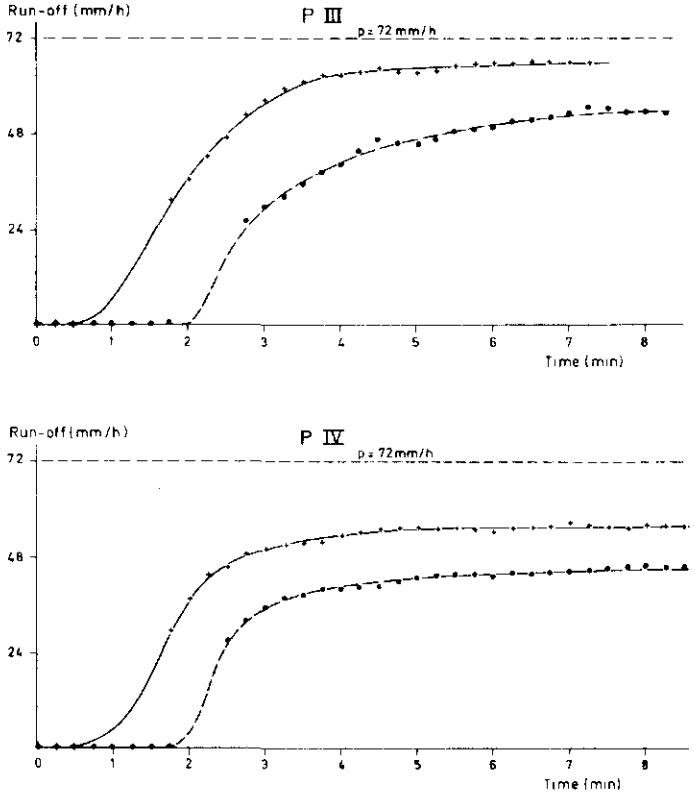

Fig. 10. Run-off hydrographs for wet and dry initial conditions at Pomona. + wet initial conditions, • dry initial conditions.

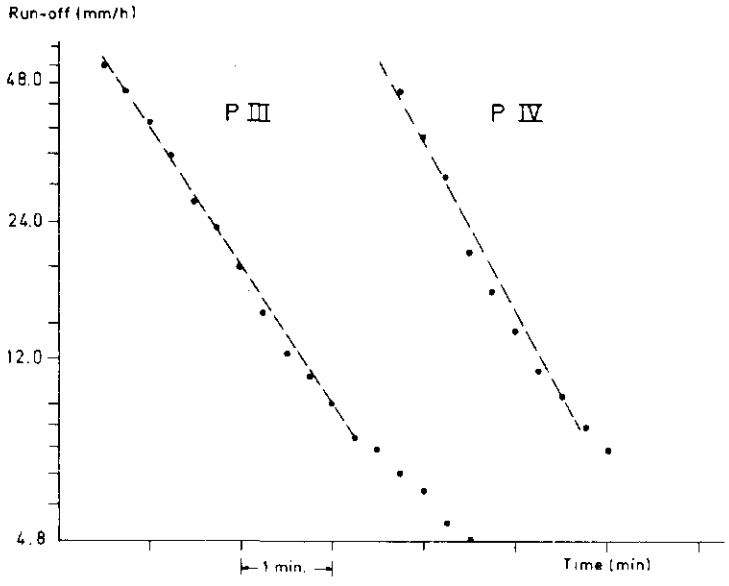

Fig. 11. Recession curves at Pomona. P III: k = 1 min 26 s, P IV: k = 1 min 12 s.

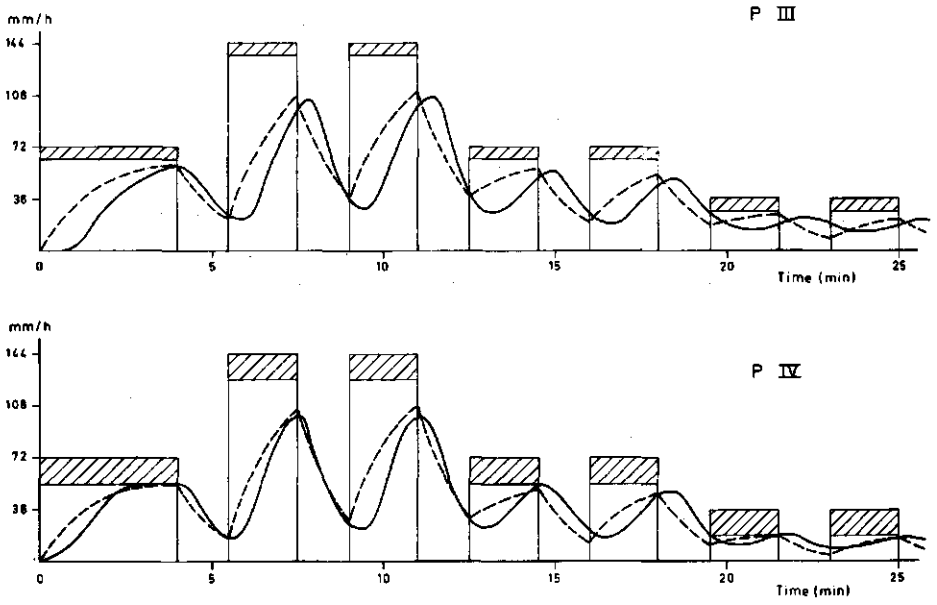

Fig. 12. Run-off simulations with the linear reservoir model. The values for the lag times were obtained from the recession curve (Fig. 11, Pomona). ⎍ rainfall, ▨ infiltration, — observed run-off, – – – simulated run-off. P III: k = 1 min 26 s, P IV: k = 1 min 12 s.

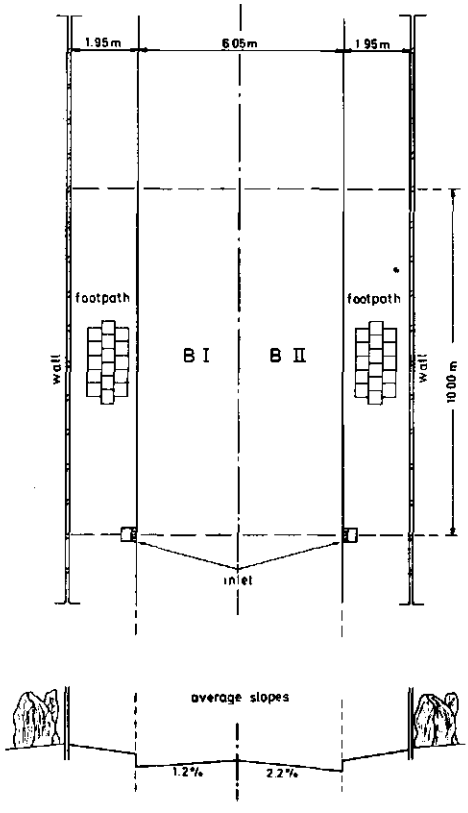

Fig. 13. Plan of the road at Bennekom.

basis of a best fit between a measured run-off hydrograph and a hydrograph that is reconstructed with the corresponding effective rainfall when using a linear time-invariant model:

– Correct the rainfall for some showers according to both loss-models.
– Identifications of the catchment area for each shower, either with a blackbox model or with a conceptual model.
– Reconstruct run-off hydrographs and select the loss model that provides the best fits.

In this way van Gastel (1976) found for the Gray Haven catchment area that loss model A+C yielded more consistent results than model A+B. A comparison of conceptual

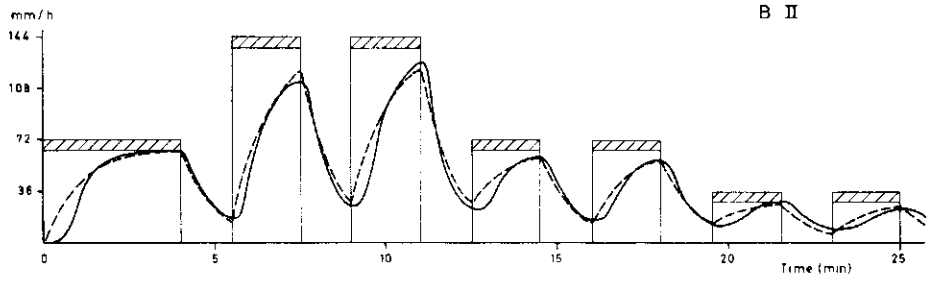

Fig. 14. Run-off simulation with the linear reservoir model. The value for the lag time was obtained from the recession curve of the Bennekom data. k = 1 min. ⎍ rainfall, ▨ infiltration, — observed run-off, – – – simulated run-off.

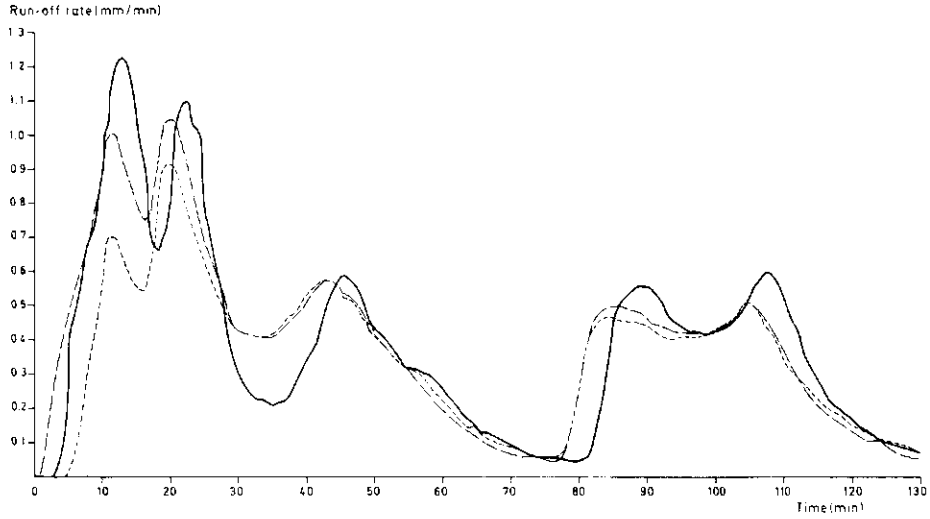

Fig. 15. Run-off simulations with the Nash cascade for Event A23 from Table 2 (Gray Haven). The model parameters were estimated by moment fitting for Storm 7 from Table 3 for the loss models initial loss + Φ index and initial loss + proportion assumed lost, — observed run-off, – – – proportion assumed lost, ----- Φ index.

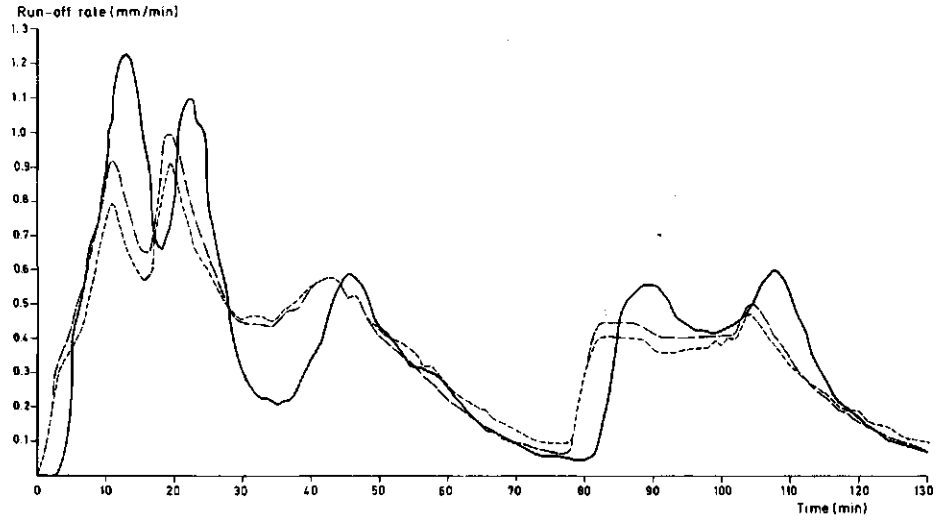

Fig. 16. Run-off simulations with the Nash cascade for Event A23 from Table 2 (Gray Haven). The model parameters were estimated by moment fitting for Storm 8 from Table 3 for the loss models Φ index and proportion assumed lost. — observed run-off, – – – proportion assumed lost, ----- Φ index.

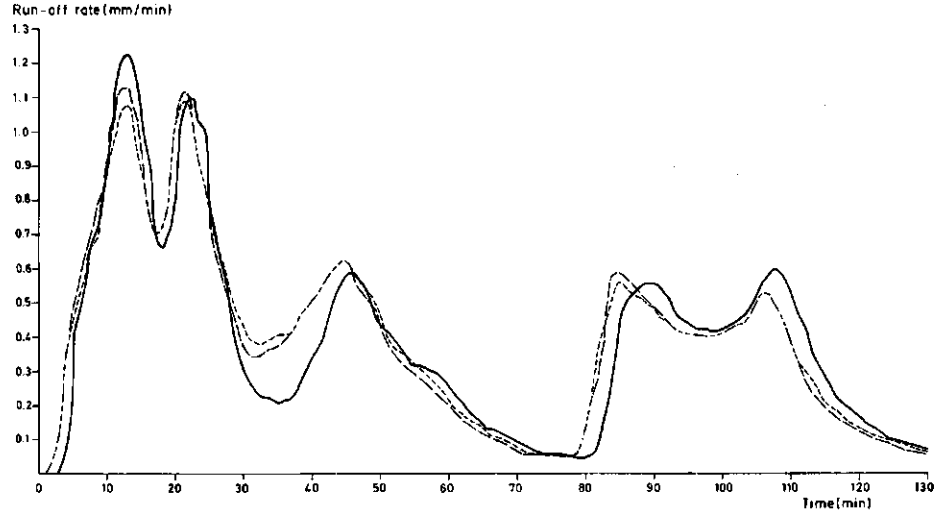

Fig. 17. Run-off simulations with the model convective diffusion, upstream inflow, for Event A23 from Table 2 (Gray Haven). The model parameters were estimated by moment fitting for Storm 7 from Table 3 for the loss models initial loss + Φ index and initial loss + proportion assumed lost. — observed run-off, – – – proportion assumed lost, ----- Φ index.

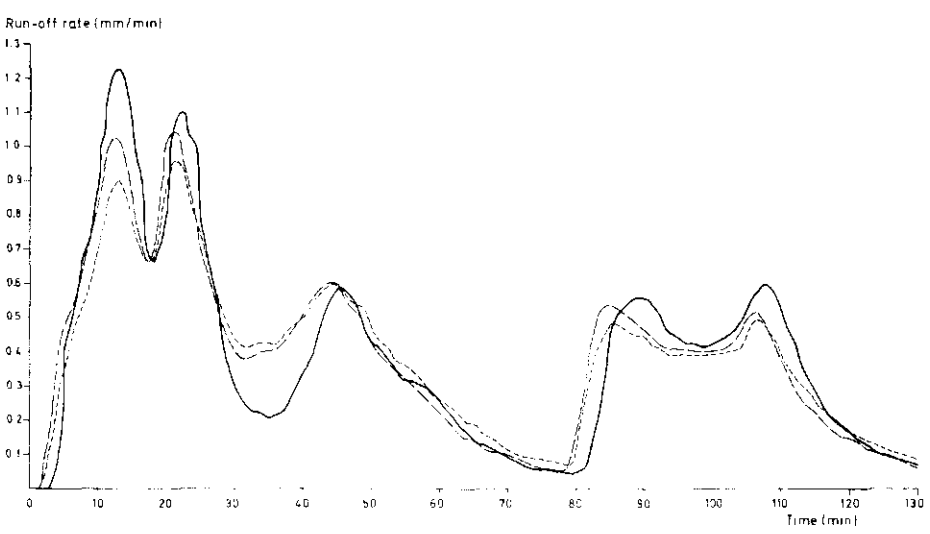

Fig. 18. Run-off simulations with the model convective diffusion, upstream inflow, for Event A23 from Table 2 (Gray Haven). The model parameters were estimated by moment fitting for Storm 8 from Table 3 for the loss models Φ index and proportion assumed lost. — observed run-off, – – – proportion assumed lost, ----- Φ index.

models for transformation of net rainfall into sewer run-off in this catchment area (Chap. 6) indicated that the best models were the Nash cascade and the convective diffusion model with upstream inflow. For these two models, van Gastel estimated the parameters by moments for two showers (No 7 and 8 of Table 3 (Chap. 5)). For both showers, the losses were distributed according to the loss models A+B and A+C, respectively. With the parameters obtained, he simulated the outflow of event A23 of Table 2 (Chap. 5), which was chosen because of the many sharp peaks and good water balance (Fig. 15-18). With both conceptual models abstraction of losses by model A+C yielded hydrographs which better corresponded to the measured run-off than modelling of losses with A+B.

4 Transformation of net rainfall into run-off

4.1 Linearity and time invariance of catchment areas

In hydrology, linear time-invariant models are widely used. The reason for this preference is the wealth of mathematical methods available for analysis of linear systems. The final judgment of their applicability, however, must be based on closeness to linearity and to time invariance of the systems behaviour.

Because of the effect of previous rainfall, all catchments, both urban and non-urban, will be non-linear and time-variant (Chap. 3). This problem is usually solved by representing rainfall run-off by a series of two subsystems. The first subsystem concerns the subtraction of losses and the second subsystem transforms the net or effective rainfall into catchment run-off. The effect of previous rainfall is thus expressed in the loss model, and for the transformation model the assumption of linearity and time invariance is usually maintained.

The second subsystem can then be characterized by its impulse response, which in hydrology is usually called the Instantaneous Unit Hydrograph (IUH)[1]. A number of case studies, however, point out (Chap. 5; also Childs, 1958; Minshall, 1960; Singh, 1964; Pilgrim, 1966) that the form of the IUH is not always the same for different events. In the case studies, the heavier the analysed storm, the higher was the peak of IUH and the smaller the time to peak of IUH.

4.2 Some approaches to modelling of non-linear catchment areas

Because of the results in Section 4.1, investigators searched for models to describe the second subsystem adequately, taking the observed non-linear behaviour into account. Two approaches can be distinguished:

1. A more general non-linear theory replaces the linear theory, in which the output $q(t)$ from a linear system can be expressed by convolution-integration of the kernel function $h(t)$ with the system input $p(t)$:

$$q(t) = \int_0^\infty h(\tau)\, p(t-\tau)\mathrm{d}\tau \; ; h(\tau) = 0 \text{ for } \tau > t \tag{4.1}$$

1. In numerical calculations, one frequently uses the pulse response (unit hydrograph). When the time interval used to determine the unit hydrograph is sufficiently small, the unit hydrograph and the IUH can be considered identical.

where $h(\tau)$ stands for the instantaneous unit hydrograph.
This is only the first term of the representation of the non-linear case by the functional series (Amorocho & Orlob, 1961)

$$q(t) = \int_0^\infty h_1(\tau)p(t-\tau)d\tau + \int_0^\infty \int_0^\infty h_2(\tau_1, \tau_2)p(t-\tau_1)p(t-\tau_2)d\tau_1 d\tau_2 + \ldots +$$

$$+ \int_0^\infty \ldots \int_0^\infty h_n(\tau_1, \ldots, \tau_n)(p(t-\tau_1)\ldots p(t-\tau_n)d\tau_1 \ldots d\tau_n + \ldots \qquad (4.2)$$

with $h(\tau) = 0$ for $\tau > t$.
Mathematical complications. however, make practical applications in which more than the first term of Equation 4.2 are used rater complicated. An abbreviated version of this approach was introduced by Diskin & Boneh (1972).
2. In the approach that some authors call 'quasilinear' (e.g. Delleur & Rao, 1973; Diskin, 1973), it is assumed that linear theory can also be applied to non-linear catchment behaviour, if an IUH is chosen according to the size of the event. So linear behaviour within an event is assumed. Examples of this approach were given by Singh (1964) and Diskin (1973).

Singh used a conceptual model of which the parameters are a function of the storm intensity. Diskin can be cited to illustrate the line of thought in this approach: 'The instantaneous unit hydrograph may be viewed also as a distribution curve of the times of travel of all particles of water deposited on the watershed at the instant of occurrence of the impulsive rainfall input ... the time of travel is influenced by two sets of factors, one related to the topographic features of the watershed and the other to the conditions in the watershed at the time concerned.'

Diskin assumes that the first set of factors determines the 'basic shape' of the IUH, while the second set determines only the time scale of IUH. Thus the second set of factors, which determines the state of the system for one particular storm, proportionally influences the times of travel of water particles.

With this consideration, Diskin proposes a quasilinear approach and tests this approach with data from a catchment of about 0.11 km^2 in Illinois, published by Minshall (1960). Minshall clearly demonstrated the non-linear behaviour of this catchment by deriving different unit hydrographs for a number of storms of short duration and different peak intensities.

Diskin reduced the unit hydrographs as derived by Minshall to their basic shapes by multiplying the ordinates by the lag time and dividing the abscissa by the lag time. The resulting transformed hydrographs were almost identical. To use the basic shape of the unit hydrograph for simulation, information is required on the factors determining the lag time of IUH for the catchment. Diskin found that for the unit hydrographs, as derived by Minshall, the variation in shape could be explained with only one storm parameter. the average rainfall rate.

Tracer experiments by Pilgrim (1966, 1976) on travel times and non-linearity of flood run-off support the quasilinear concept. Pilgrim found that the travel time of water

particles is related to the characteristics of the whole flood wave rather than to the particular portion of the flood wave in which most of the tracer occurs. These results confirm those of Laurenson (1964) and Askew (1970), who both analysed rainfall and run-off data, and found that the lag time of the catchments was strongly correlated with the amplitude of the run-off wave.

Pilgrim suggested a quasilinear method in which the peak of run-off is used to indicate which IUH is valid for a particular rainfall event. Pilgrim further found that the time of travel decreased rapidly with increasing run-off peaks to a fairly constant value at medium to high discharges. This means a tendency towards linearity at higher run-off values.

From the relation between the lag time and the rainfall rate that Diskin derived for Minshall's data, a similar conclusion can be drawn. For storms with a low average rainfall rate, an increase in average rainfall rate corresponds with a great reduction in lag time, while for storms with a high average rainfall intensity the lag time approximates to a constant value. Besides the two approaches, described above, Dooge (1967a, 1967b) proposed a cascade of equal non-linear reservoirs with lateral inflows as a special type of non-linear model. This model has the property that once the outflow $q(t)$ for a certain input function $p(t)$ is known, the outflow for a class of 'similar' input functions can be derived from the known outflow $q(t)$. Dooge calls this property 'uniform non-linearity'. The uniform non-linear model will be illustrated in a slightly simplified form by a cascade of equal non-linear reservoirs with only inflow into the first reservoir. The differential equation for one reservoir is given by

$$\frac{dS}{dt} + a \cdot S^c = p(t) \tag{4.3}$$

where S is storage volume, $p(t)$ input, and a,c coefficients.
Two different inflow functions $p_i(t)$ and $p_j(t)$ are said to be similar if their successive rates vary in the same proportion and if the time units of the two time distributions of inflow are related to the respective intensities by

$$\frac{t_i}{t_j} = \left(\frac{p_j(t)}{p_i(t)} \right)^{\frac{c-1}{c}} \tag{4.4}$$

where t_i, t_j are time units of the inflow functions.

This property can be derived (Dooge, 1967a) by converting the set of differential equations of the model into dimensionless form, for which the proof is given in Appendix 2. Because of some properties which will now be described, a uniform non-linear model with a cascade of two non-linear reservoirs is used for comparison of some methods of the quasilinear approach, which seems simpler and more practical. Numerical experiments with this model are described in Appendix 3.

Blackbox analysis with Laguerre functions of pulse inflows and corresponding outflow waves yielded IUH of different shapes. They all were found to have the usual shape of a positively skewed wave. For waves caused by pulse inflows of the same duration but of increasing amplitude the peaks of the corresponding IUH became higher and earlier.

Outflow waves, caused by pulse inflows of the same amplitude but of increasing duration were characterized by IUH with higher and earlier peaks. Thus both the rate and duration of the inflow tended to increase the peak rates and the positive skewness of the IUH that represented the best linear approximations of the corresponding outflow waves. In the subsequent test of some quasilinear methods, the magnitude but not the duration of the event was selected as indicator for the appropriate IUH. This agrees with the general experience cited for quasilinear methods. Two quasilinear methods are compared:

1. A variant of the method used by Diskin (1973). When applying Diskin's method, the problem arises how to divide a record of rainfall and run-off data into separate run-off events. The choice of divisions determines the average rainfall rates of the single events. The rainfall rates in turn determine the choice of IUH. Therefore in the proposed variant, a running average of rainfall rate is used. For every bar of the input histogram, P_i, an IUH is chosen on the criterion

$$r_i = \frac{\sum_{j=-n}^{j=+n} P_{i-j}}{2n+1} \tag{4.5}$$

where n is dependent on the catchment. An optimum value for n must be obtained by trial and error.

A time $(2n + 1)\cdot\Delta t$, where Δt represents sampling interval of the data, can be considered as 'extent of influence'. The rainfall in this 'extent of influence' is supposed to determine the state of the system for the time that P_i is transformed into run-off.

2. The quasilinear method with the peak as proposed by Pilgrim (1976). When a hydrograph of outflow is constructed on the basis of a hyetograph of net rainfall, the peak of run-off is unknown beforehand and an iterative procedure is required.

The result of the numerical experiments on a cascade of two equal non-linear reservoirs can be summarized as follows. For durations of inflow $T = 3$ units and $T = 16$ units, the best linear transformation between calculated inflow and outflow was determined for various constant levels of inflow p. $T = 3$ was shorter and $T = 16$ longer than the four segments of an assumed 'test storm', which lasted from 4 to 7 units (Fig. A3.8). For $p \geqslant 1$, the shape of IUH for the best linear transformation approached a limiting shape if $T > 8$, because then the outflow peak approaches the inflow p.

First both quasilinear methods were tried out with IUH for $T = 16$ units. Their simulations of the run-off of a 'test storm' were compared with the 'true' computed run-off hydrograph. The proposed variant of the method of Diskin (1973), which uses rainfall rate as criterion was not successful, because no clear indications were found concerning the length of the 'extent of influence'. Pilgrim's quasilinear method, which uses the peak value of a run-off wave to select IUH, better simulated outflow than the linear method.

So only Pilgrim's method yielded promising results. Only for this method was the experiment repeated for $T = 3$ units. This time the quasilinear simulation was only slightly better than the linear simulation. For the linear method, however, IUH was chosen in accordance with the average peak of outflow, which is normally not known

when an outflow hydrograph is constructed. One can expect that for a real catchment the shape of IUH will be determined by both the duration and rate of rainfall, as conceived by Dooge as a cascade of equal non-linear reservoirs. As the peak of run-off is determined by rate and duration of rainfall, the use of the peak of run-off as criterion to select IUH seems also theoretically appropriate if one opts for a quasilinear method.

5 Case study of a small urban catchment area by a quasilinear method

5.1 Catchment description

Data from a small urban catchment area in the town of Gray Haven (Fig. 19), which lies about seven miles east of Baltimore, Maryland, United States, are used for a case study to test the quasilinear approach based on the peak rates of run-off.

Tucker (1969) published data on rainfall and sewer run-off for 29 rainfall events on this urban catchment area. The sampling interval of the data was one minute. The catchment area is 94 300 m^2 and consists of a homogeneous residential area with 'group houses' on lots of about 250 m^2. Of the catchment area, 52% can be considered impervious. Pervious parts of the catchment area are undergrass, the sod being underlain by sandy soil Ground slopes in the catchment area are gentle, averaging about 0.5%. Synchronized data on rainfall and run-off were collected from 1962-1967 with a tipping bucket raingauge and a Parshall flume, respectively.

Because the subsoil is sandy, one can expect that the pervious part only seldom contributes to the sewer run-off, because of a high infiltration capacity.

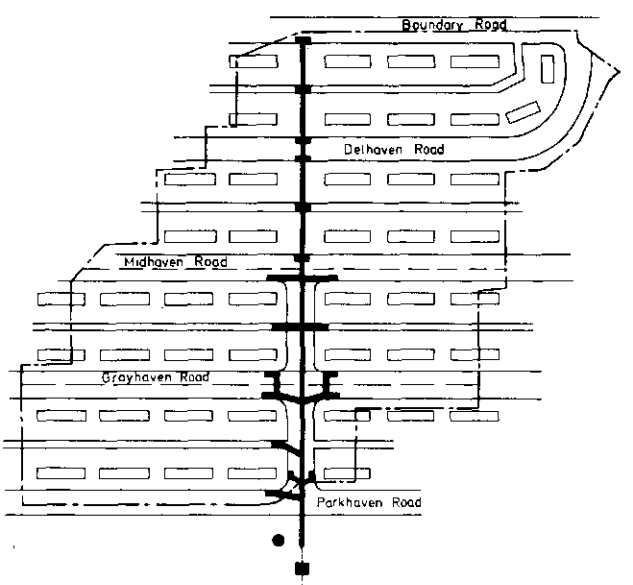

Fig. 19. Plan of the Gray Haven catchment area. —·— catchment boundary, • raingauge, ▪ Parshall flume, ▬ drainage system.

5.2 Analysis

Of Tucker's original series of 29 events, 3 events had to be discarded as duplicate data from different sources. Of the remaining 26, the records of 5 events were incomplete. This reduced the number to 21 events. A further screening of the records was necessary to eliminate those where the recorded run-off as related to the impervious area, exceeded the recorded depth of rainfall. This is explained below.

To make a water balance for each event, records that had been cut off before sufficiently low run-off values had to be fitted with an artificial 'recession tail'. Such a recession tail could also serve to split composite waves into separate events. Table 2 gives water balances for 21 events, assuming that only the impervious surfaces produced sewer run-off. It shows that for three events run-off exceeded rainfall, so the events were discarded. The excess could be ascribed to either run-off from pervious surfaces or to overestimation of the average rainfall depth on the catchment area by the recorded rainfall depth. The analysis was confined to the relation between rainfall and run-off for the impervious part of the Gray Haven catchment area. Of the remaining 18 events, 8 had a run-off peak > 0.28 mm/min. These were considered as major events. Of these 8 events, 6 were used for identification and two disregarded because of excessive losses ($> 40\%$). These high 'losses' can be ascribed to either strong wind effects around the raingauge or to strong spatial variability of rainfall, both resulting in a poor representation of rainfall

Table 2. Water balance for 21 rainfall events in Gray Haven, United States, assuming that only the impervious surfaces produce sewer run-off.

Event	Rainfall	Sewer run-off	Losses	
	(mm)	(mm)	(mm)	(%)
A6	2.03	0.94	1.09	54
A7	7.87	3.76	4.11	52
A9	11.43	2.70	8.73	76
A10	7.87	4.47	3.40	43
A11	4.32	1.17	3.15	73
A12	4.32	1.44	2.88	67
A13	7.62	1.99	5.63	74
A14	11.94	6.20	5.74	48
A17	7.37	7.84	– 0.47	– 6
A18 = A1	55.88	72.05	–16.17	–29
A19 = A2	37.08	28.83	8.25	22
A20	30.23	26.01	4.22	14
A21	8.13	3.83	4.30	53
A22	15.49	9.62	5.87	38
A23 = A4	58.93	53.88	5.05	9
A24	11.43	5.83	5.60	49
A25	34.01	22.31	11.70	34
A26	13.21	11.26	1.95	15
A27	6.10	3.39	2.71	44
A28	7.62	9.78	– 2.16	–28
A29	5.59	3.71	1.88	34

by the raingauge. Of the 10 remaining minor events, 3 were selected for identification.

Before identification, effective rainfall must be determined by a proper distribution of the losses as found from the water balance. Some events were preceded by a dry period of at least 12 h. It was assumed that these events occured on initially dry pavements. By application of hydrograph simulation (Chap. 3), trial and error showed that for the events A18, A19, A20 and A23 an initial loss of 3.05 mm (0.12 inch) was appropriate.

Because correlations between the losses during an event and characteristics of that event did not provide any clue for a more detailed loss model, losses in any minute were assumed to be proportional to rainfall rate at that time after subtracting any initial loss (Chap. 3).

The method selected to identify the second subsystem (Chap. 4) was expansion of the histogram of rainfall minus losses, the run-off hydrograph and IUH in a finite number of Laguerre functions. A description of this method is given in Appendix 1.

Garvey (1972) and Dooge (1974) show that among the linear identification techniques the use of Laguerre functions or its discrete analogue the Meixner functions gives the best results for real (i.e. error-containing) data. For identification of the 9 events, 20 Laguerre functions were used to approximate input histogram and run-off hydrograph. A time-scale factor was used (Appendix 1) such that two sample intervals coincided with one time unit.

Approximations of functions with a chosen number of Laguerre functions are better as these functions have a simpler form. Therefore sometimes only the most significant part of an event was used for identification. Table 3 gives some characteristics of the

Table 3. Identification of nine selected storms (Gray Haven, United States).

Storm	Event	Rainfall (mm)	Run-off (mm)	Peak run-off rate (mm/min)	Computed loss (mm)		$\int_0^{\infty} h(t)dt$
					initial	proportional	
1	A29	5.59	3.71	0.23		1.88	0.97
2	A13 0–24 min	7.62	5.63	0.10	3.05	2.58	1.01
3	A6	2.03	0.94	0.05	1.07		0.99
4	A23 76–133 min	17.47	17.87	0.53 0.60		−0.40	1.00
5	A26 75–110 min	7.19	6.46	0.43		0.73	1.00
6	A22 25–60 min	11.46	7.68	0.39		3.78	1.02
7	A19	37.08	28.87	1.03 0.78	3.05	5.16	1.00
8	A25 191–280 min	15.54	12.89	0.58		2.65	0.98
9	A20 0–40 min	20.32	15.83	0.94	3.05	1.44	1.00

identifications; the period of rainfall used for identification is given in the second column.

The nine resulting IUH differed considerably. Heavy storms resulted in IUH with high and early peaks, thus indicating non-linear behaviour of the catchment area. The nine IUH were divided into three classes, a low, a medium and a high class (Fig. 20-22).

Figure 23 illustrates for Storm 8 from Table 3 the approximation of the input histogram and the run-off hydrograph with 20 Laguerre functions. Figure 24 compares the observed run-off hydrograph with the reconstructed run-off hydrograph after convolution-integrating the net rainfall with the derived IUH from Figure 22. Apparently linear identification was highly successful, while Figure 20-22 showed IUH depending on the

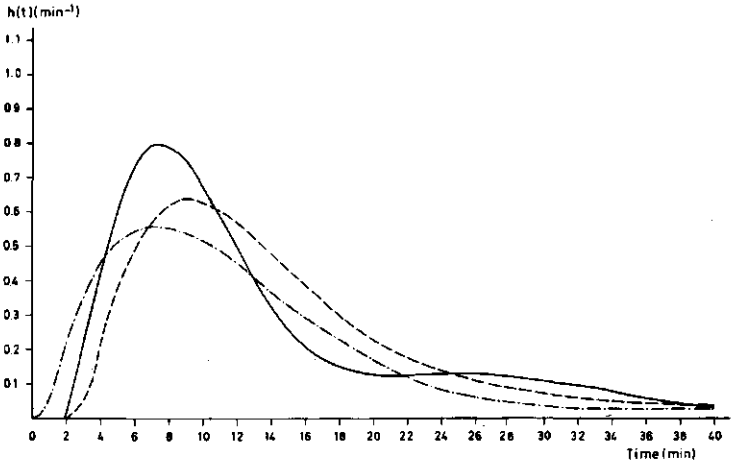

Fig. 20. Instantaneous unit hydrographs, $h(t)$, of low class. — Storm 1, – – – Storm 2, –·– Storm 3.

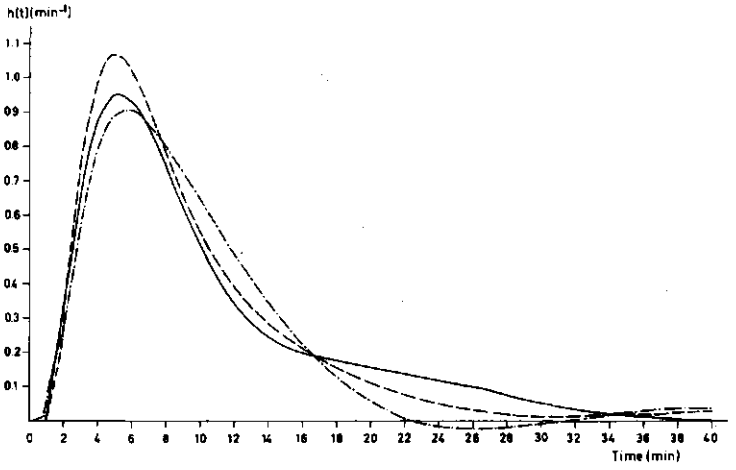

Fig. 21. Instantaneous unit hydrographs, $h(t)$, of medium class. — Storm 4, – – – Storm 5, –·– Storm 6.

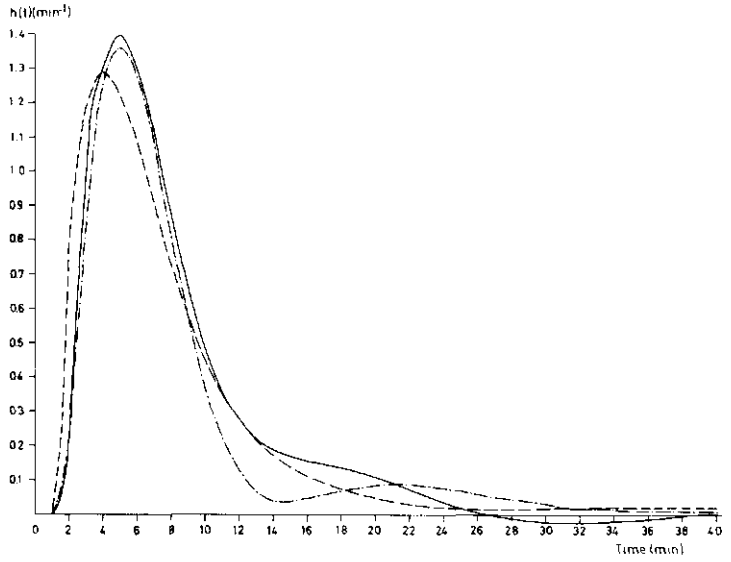

Fig. 22. Instantaneous unit hydrographs, $h(t)$, of high class. — Storm 7, – – – Storm 8, –·– Storm 9.

size of an event. This confirms the suitability of the quasilinear approach as discussed in Chapter 4. The method based on peak rates of run-off was chosen to model the Gray Haven catchment area.

This method requires the following tools:

1. For each of the 9 storms the peak q_p of the run-off hydrograph was plotted against the time to peak t_p of IUH derived for that storm. The nine points were fitted with the regression equation:

$$\lg t_p = a + b \lg q_p + c (\lg q_p)^2 \tag{5.1}$$

where a, b and c are coefficients. This arbitrary equation proved to give a satisfactory fit (Fig. 25). Values of the coefficients were a 0.651, b –0.308 and c –0.091.

2. A relation between the peak of the IUH, U_p, and the time to peak of the IUH, t_p, was determined as the hyperbola $U_p \cdot t_p = 5.57$ which corresponds with the average value for the 9 events (Fig. 26).

3. As Storm 6 yielded a point very close to this hyperbola ($U_p \cdot t_p = 5.52$), that storm was chosen to derive a basic shape for IUH (Fig. 27). So the ordinate of IUH of this storm was multiplied by the time to peak t_p and the abscissa time divided by t_p. To correct for undesirable oscillations, the tail was corrected with the IUH for Storms 4 and 5.

For verification of this quasilinear model, Event A23 (Table 2) was selected. As the IUH of Storm 4 can be considered as average IUH for the catchment area, the run-off simulation obtained by convolution-integrating the histogram of net rainfall with IUH of that storm can be used to compare the linear method with the quasilinear method. For application of the quasilinear method, the histogram of net rainfall (Fig. 28) was divided into three segments: t = 0-18, t = 18-30 and t = 30-75 min.

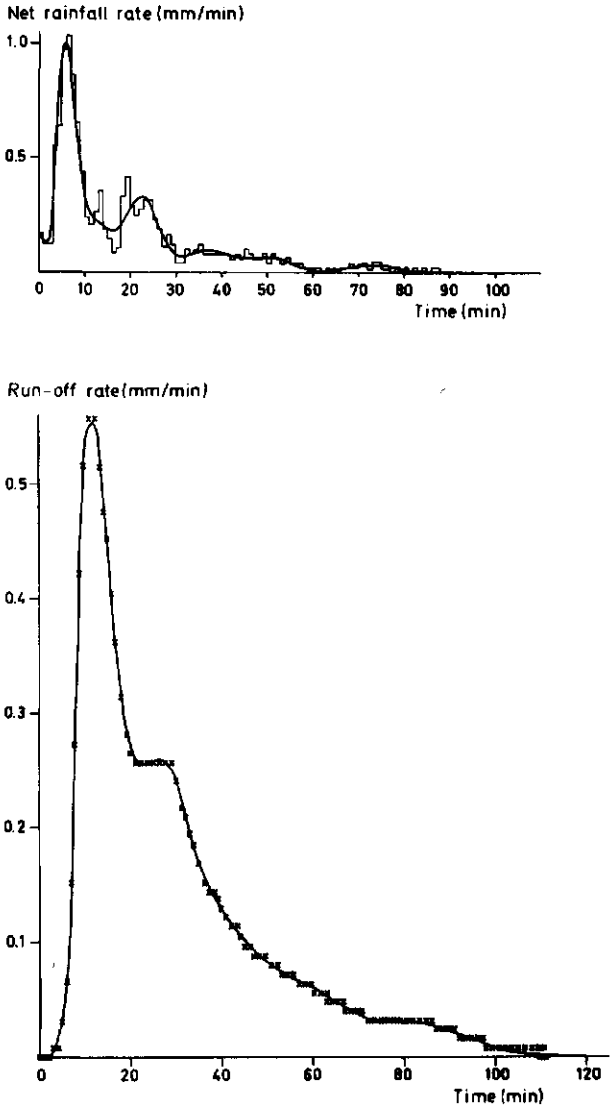

Fig. 23. Description of net rainfall rate, $p(t)$, and run-off rate, $q(t)$, with 20 Laguerre functions. observed net rainfall, — calculated net rainfall; x observed run-off, — calculated run-off.

To derive the IUH for each segment, three values for the time to peak, t_p were required. To obtain these three values, estimates for the three run-off peaks must be calculated. The peaks of run-off from the linear solution were chosen. After deriving and convolution-integrating each IUH with corresponding segments of the histogram of net rainfall, the run-off hydrograph was obtained by superimposing these three partial run-off simulations (Fig. 28). Figure 28 shows that iteration of the procedure gave only a small difference. Simulation with the quasilinear model was considerably better than linear simulation. The real initial loss was probably slightly greater than 3.05 mm (0.12 inch).

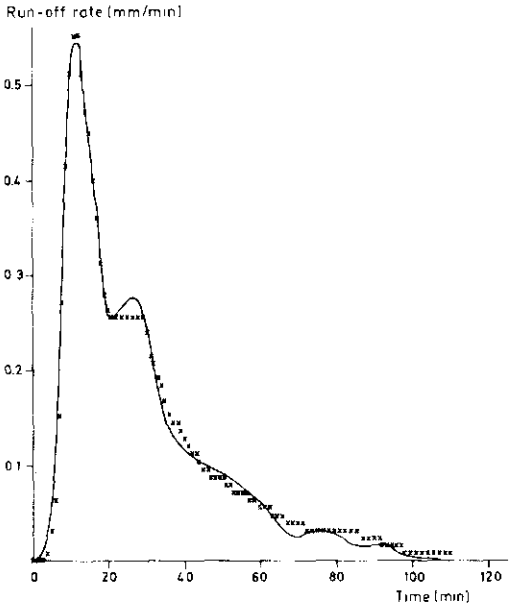

Fig. 24. Reconstruction of run-off rate for Storm 8. x observed run-off, — reconstructed run-off.

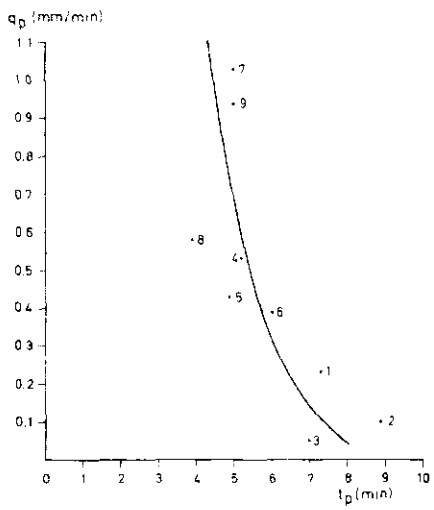

Fig. 25. Relation between the peak run-off rate, q_p, and the time to peak of the IUH, t_p.

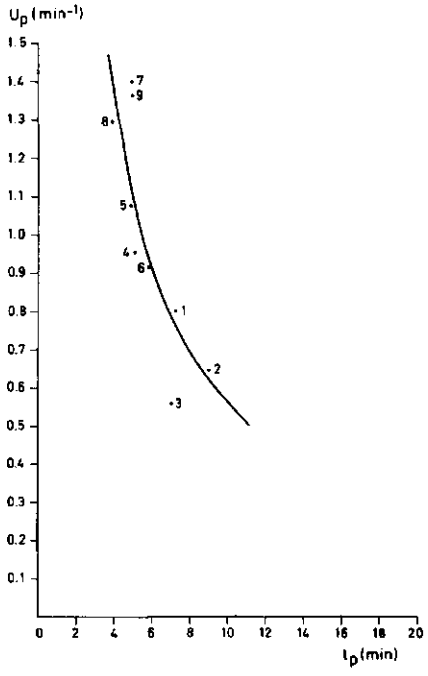

Fig. 26. Relation between the peak of the instantaneous unit hydrograph, U_p, and the time to peak of the IUH, t_p.

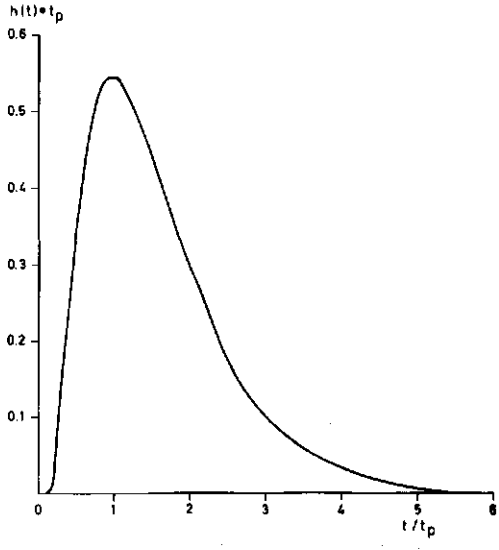

Fig. 27. Basic shape of IUH.

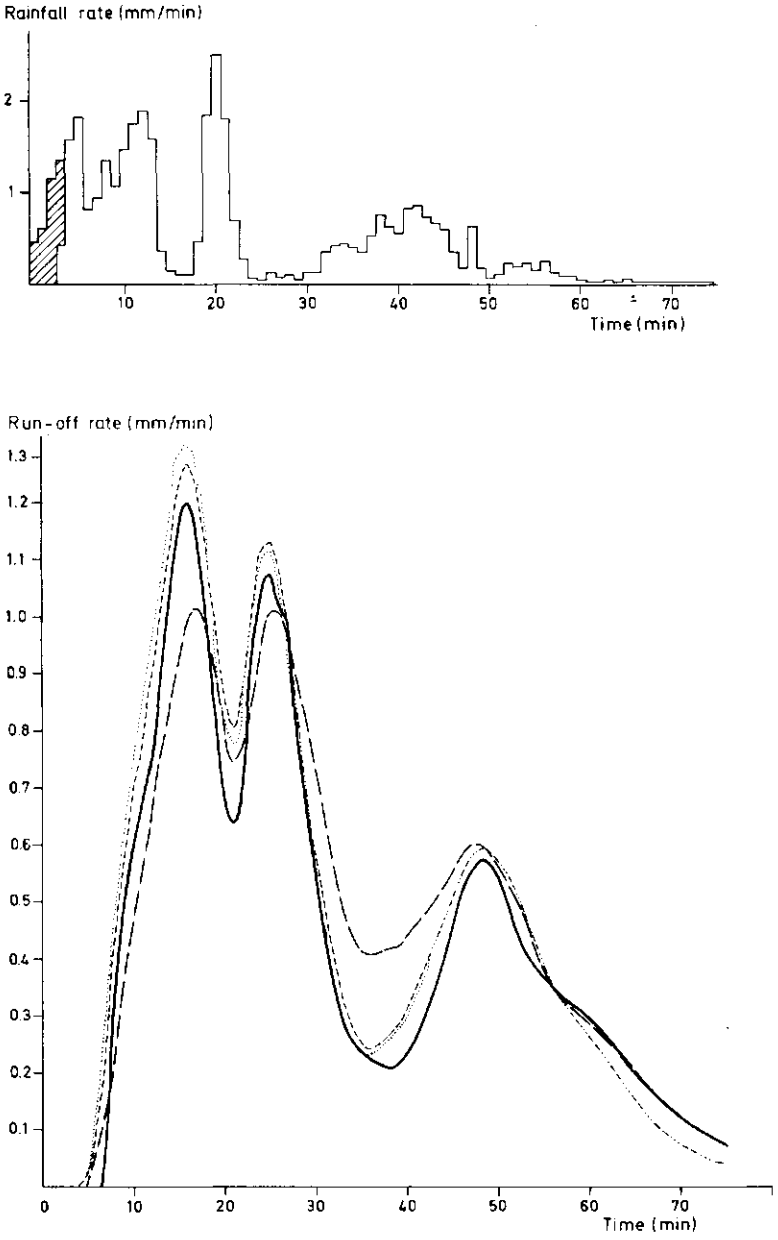

Fig. 28. Linear and quasilinear simulations of run-off for Event A23. ▨ losses, — observed run-off, – – – linear simulation, ----- quasilinear simulation (first time), ····· quasilinear simulation (second time). Sum of squared differences: linear simulation 0.87 mm^2/min^2, quasilinear simulation 0.46 mm^2/min^2.

6 Quasilinear approach with conceptual models

6.1 Linear conceptual models

An alternative application of the proposed quasilinear approach is a linear conceptual model instead of the general linear model with Laguerre functions. For such an application, a linear conceptual model must be chosen. Viessman (1966) found the linear reservoir suited to model rainfall and sewer run-off of four small impervious urban catchment areas (area 1600-4000 m^2). Sarma et al. (1973) found the Nash cascade a good model to use on larger urban areas.

Six conceptual models were compared for the Gray haven catchment area, according to LS:

1. Linear reservoir. For the linear reservoir, run-off rate is proportional to storage volume:

$$S = k \cdot q \tag{6.1}$$

where k is lag time of the reservoir, q is run-off rate and S is storage volume. The IUH of this model is given by

$$h(t) = \frac{e^{-t/k}}{k} \tag{6.2}$$

2. Time shift plus a linear reservoir ('lag-and-route'). The IUH of this model is:

$$\text{if } t > \tau \text{ , } h(t) = \frac{e^{-(t-\tau)/k}}{k} \tag{6.3}$$
$$\text{if } \tau > t > 0 \text{ , } h(t) = 0$$

where τ is time shift.

3. Cascade of a j model and a linear reservoir. The j model is a diffusion model and was derived for groundwater flow to parallel ditches (Kraijenhoff van de Leur, 1958). The IUH of the cascade model can be obtained by convolution-integrating the IUH of the j model with the IUH of the linear reservoir. The IUH of the j model is as follows:

$$h(t) = \frac{8}{\pi^2 \cdot j} \sum_{n=1,3,\ldots}^{n=\infty} e^{-n^2 t/j} \tag{6.4}$$

where j is reservoir coefficient.

So for a cascade of a j model and a linear reservoir, one finds

$$h(t) = \frac{8}{\pi^2}\left[\frac{1}{j-k}\left(e^{-t/j} - e^{-t/k}\right) + \frac{1}{j-9k}\left(e^{-9t/j} - e^{-t/k}\right) + \right.$$

$$\left. + \frac{1}{j-25k}\left(e^{-25t/j} - e^{-t/k}\right) + \ldots\right] \tag{6.5}$$

4. Nash cascade (Nash, 1959). The IUH of this model, which consists of a cascade of v equal reservoirs with lag time k, is as follows:

$$h(t) = \frac{1}{k.\Gamma(v)}\, e^{-t/k}\, \left(\frac{t}{k}\right)^{v-1} \tag{6.6}$$

where $\Gamma(v)$ is gamma function.

5. Convective diffusion analogy with upstram inflow or (6) partial lateral inflow. These models are based on the partial differential equation:

$$\frac{\partial q}{\partial t} = D\frac{\partial^2 q}{\partial x^2} - \frac{A_\tau \partial q}{\partial x} \tag{6.7}$$

where A_τ is translation coefficient, D diffusion coefficient and q run-off. The diffusion Equation 6.7 can be considered as a simplification of the differential equation for non-steady flow in an open channel (Schönfeld, 1948; Hayami, 1951).

For a channel infinite in one direction, with inflow at the upstream end, for a point at a distance l from this end, IUH is as follows (Harley, 1970):

$$h(t) = \frac{H\sqrt{I}}{\sqrt{2\pi t^3}}\, e^{-\left(\frac{H\sqrt{I}}{\sqrt{2}} - \frac{1}{\sqrt{2I}}t\right)^2 / t} \tag{6.8}$$

where $H = (l \cdot A_\tau)/2D$ (dimensionless length parameter) and $I = 2D/A_\tau^2$ (characteristic time parameter).

Considering a section of lenght l of an infinite channel, van de Nes (1973, Eq. 4.33) gave IUH for the downstream end of this section, for lateral inflow over a length m (Fig. 29) as (here slightly adapted):

$$h(t) = \frac{1}{2G\cdot H\cdot I}\left[\operatorname{erf}\left(\frac{H - t/I}{\sqrt{2t/I}}\right) - \operatorname{erf}\left(\frac{H(1-G) - t/I}{\sqrt{2t/I}}\right)\right] +$$

$$+ \frac{1}{2G\cdot H\cdot I}\,\frac{1}{\sqrt{2\pi t/I}}\left[e^{\frac{-(H(1-G) - t/I)^2}{2t/I}} - e^{\frac{-(H - t/I)^2}{2t/I}}\right] \tag{6.9}$$

where $G = m/l$.

In computations, the summation in Equation 6.5 was truncated after the seventh term. For computation of Equation 6.9 the following approximation was used for the error functions (Abramowitz & Stegun, 1965):

$$\operatorname{erf} x = 1 - (a_1 w + a_2 w^2 + a_3 w^3 + a_4 w^4 + a_5 w^5)\ e^{-x^2} + e(x) \qquad (6.10)$$

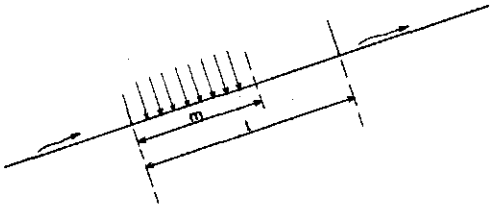

Fig. 29. Partial lateral inflow into a section of an infinite channel. *m*, length over which inflow takes place; *l*, total length considered.

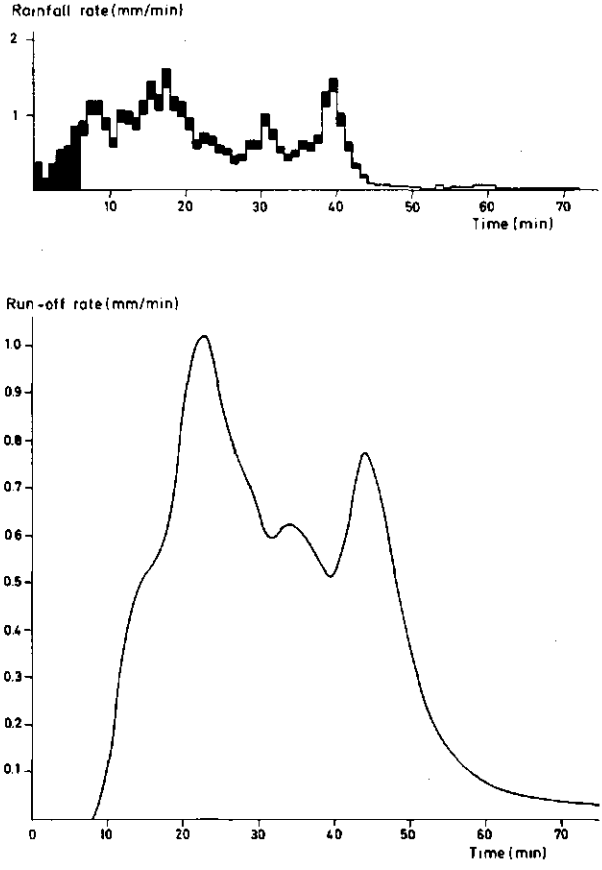

Fig. 30. Rainfall and run-off for Storm 7. ▪ subtraction of losses.

if $x > 0$, where $w = 1/(1 + z \cdot x)$, $|e(x)| \leqslant 15 \times 10^6$, and

$z = 0.3275911$
$a_1 = 0.254829592$
$a_2 = -0.284496736$
$a_3 = 1.421413741$
$a_4 = -1.453152027$
$a_5 = 1.061405429.$

To obtain a logical comparison of the models, some storms of the same class must be used. Because heavy rainfall is most interesting, Events 7 and 8 of Table 3 were selected to optimize the parameters of the six models. After correction for losses (Fig. 30 and 31) the parameters of the six models were optimized for LS. For this, a computer program of a 'direct-search method' was used. For optimization of the parameters of the cascade of a j model with a linear reservoir, one must be prepared for the appearance of two extremes.

Characteristic shapes of the sum of squared differences between measured and simulated run-off as function of model parameters were given for some models by Zondervan & Dommerholt (1975). Results of the parameter optimizations are given in Table 4, which shows that the lag-and-route model, the Nash cascade and the two diffusion models best approach the run-off curves. The parameter G of the model with lateral inflow approached zero, which means that the limiting case 'tributary inflow' holds.

Van de Nes (1973, p.79) shows that for $H \geqslant 1.8$ the shapes of IUH for tributary inflow and upstream inflow are almost identical. Then, where $H = 3$ the difference in performance between the two models can be neglected.

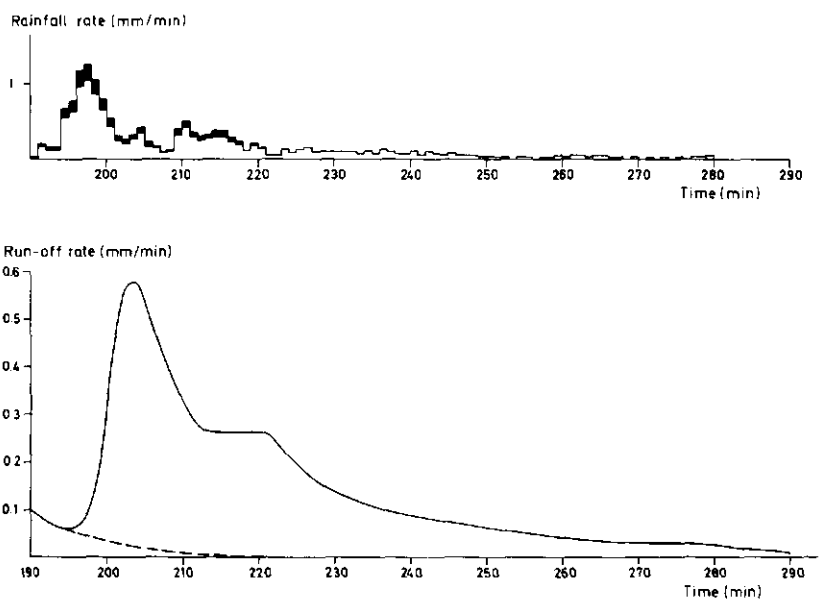

Fig. 31. Rainfall and run-off for Storm 8. ▪ subtraction of losses, —— separation from previous run-off wave.

Table 4. Results of parameter optimization with two storms of the high class (Gray Haven, United States).

Model	Storm 7		Storm 8	
	optimized parameters	LS (mm^2/min^2)	optimized parameters	LS (mm^2/min^2)
Linear reservoir	k = 8.51 min	0.59	k = 9.99 min	0.34
Time shift + linear reservoir	τ = 3 min k = 5.37 min	0.05	τ = 4 min k = 4.85 min	0.03
j model + linear reservoir	j = 3.72 min k = 4.82 min	0.27	j = 3.85 min k = 5.34 min	0.16
Nash cascade	ν = 3.26 k = 2.40 min	0.10	ν = 4.00 k = 1.97 min	0.04
Convective diffusion, upstream inflow	H = 2.76 I = 2.95 min	0.06	H = 3.27 I = 2.56 min	0.03
Convective diffusion, partial lateral inflow	G = 0.01 H = 3.00 I = 2.32 min	0.07	G = 0.01 H = 3.50 I = 2.08 min	0.03

Table 5. Results of run-off simulations for Event A23 with parameter values as found for Storm 7 and 8 (Gray Haven, United States).

Model	Parameters Storm 7			Parameters Storm 8		
	sum of squared differences (mm^2/min^2)	simulated peaks (mm/min)		sum of squared differences (mm^2/min^2)	simulated peaks (mm/min)	
Linear reservoir	1.23	0.95 +0.26	1.04 −0.04	1.32	1.05 −0.16	1.11 +0.03
Time shift + linear reservoir	0.87	1.35 +0.14	1.31 +0.23	0.22	1.30 +0.09	1.27 +0.19
j model + linear reservoir	0.53	0.99 +0.22	1.03 −0.05	0.51	1.04 −0.17	1.04 −0.04
Nash cascade	0.45	1.24 +0.03	1.07 −0.01	0.33	1.19 −0.02	1.07 −0.01
Convective diffusion, upstream inflow	0.38	1.24 +0.03	1.13 +0.05	0.22	1.23 +0.02	1.14 +0.06
Convective diffusion, partial lateral inflow	0.37	1.24 +0.03	1.12 +0.04	0.22	1.23 +0.02	1.13 +0.05

Next the run-off from the teststorm of Chapter 5 was simulated with the parameter values from Table 4. Results are given in Table 5. The three models with the best fit for optimization as given in Table 4 also yield the best simulation. The Nash cascade and the diffusion models give the smallest error for peak-flows. Convective diffusion with upstream inflow was selected for use with the quasilinear method. The IUH of this model is simpler than the IUH of the Nash cascade, while experience with this model and the Nash cascade showed an easier optimization.

6.2 Application of a quasilinear method on a small urban catchment area, using a conceptual model

For application of the quasilinear approach with use of a conceptual model, first the two parameters of the chosen model, the convective diffusion analogy with upstream inflow, were optimized by LS for the 9 storms (Table 3). The parameter values are given in Table 6.

Table 6. Optimized parameter values of the model convective diffusion, upstream inflow. The parameters are optimized by LS.

Class	Storm	H	I (min)	$H \cdot I$ (min)	Average lag time $(\overline{H \cdot I})$ (min)
Low	1	2.31	6.16	14.23	15.2
	2	2.55	5.95	15.17	
	3	1.65	9.79	16.15	
Medium	4	2.28	4.94	11.29	10.5
	5	2.19	4.46	9.76	
	6	3.43	3.03	10.42	
High	7	2.76	2.95	8.13	8.01
	8	3.27	2.56	8.37	
	9	1.76	4.35	7.67	

Next a relation between the peak run-off rate q_p and a characteristic time of IUH was determined. As characteristic time, the lag time of the IUH t_l was chosen, which can easily be computed as the product of the two parameters of the model:

$$t_l = H \cdot I \tag{6.11}$$

As in Chapter 5, the regression formula $\lg t_l = a + b \lg q_p + c(\lg q_p)^2$ with a, b, c : coefficients was used to fit the points of the nine storms (Fig. 32). Values of the coefficients were a 0.891, b −0.422 and c −0.133. The relation between the peak of the IUH, U_p, and the lag time of the IUH, t_l, was determined from the hyperbola $U_p \cdot t_l$ as 0.984 (Fig. 33).

A basic shape of IUH was derived from the IUH for Storm 7 (Fig. 34), which yielded a point very close to the hyperbola of Figure 33 ($U_p \cdot t_l = 0.984$). To test the model, Event

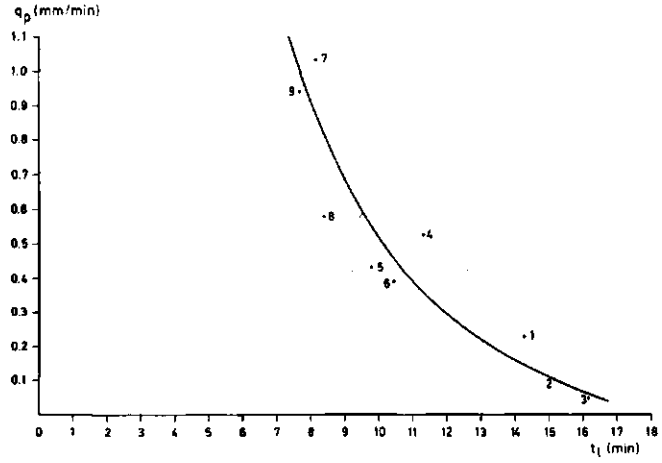

Fig. 32. Relation between peak run-off rate, q_p, and lag time of IUH, t_l.

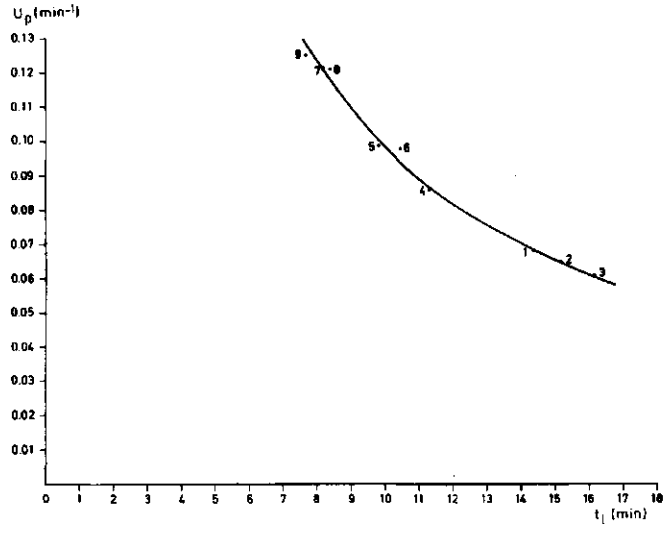

Fig. 33. Relation between the peak of the IUH, U_p, and the lag time of IUH, t_p.

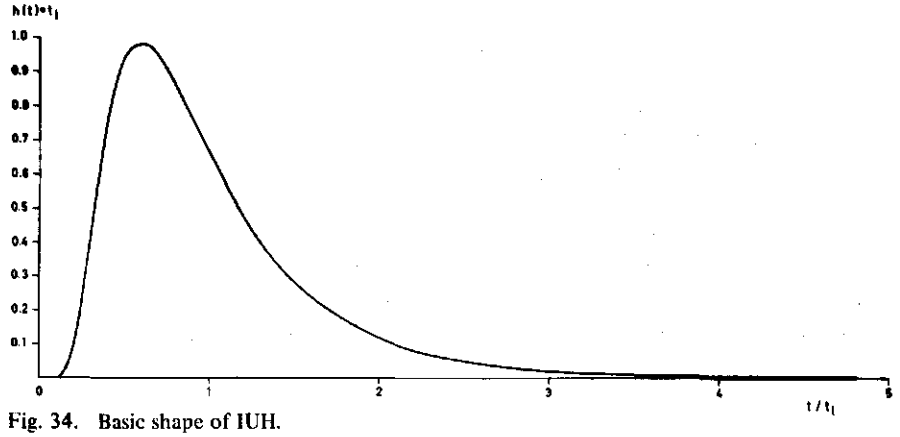

Fig. 34. Basic shape of IUH.

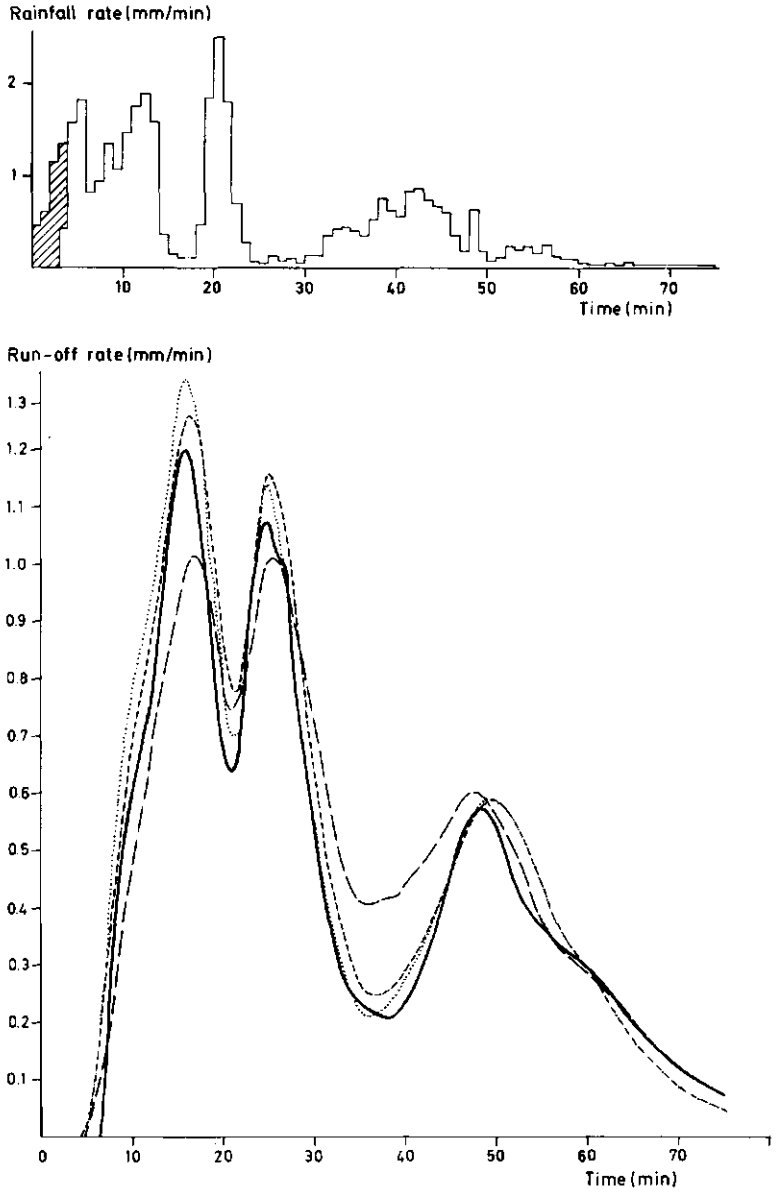

Fig. 35. Quasilinear simulation of run-off for Event A23. ▨ losses, — observed run-off, – – – linear simulation, ----- quasilinear simulation (first time), ····· quasilinear simulation (second time). Sum of squared differences: linear simulation 0.87 mm^2/min^2, quasilinear simulation 0.30 mm^2/min^2.

A23 was again used. The simulated peak values of the linear approach (obtained with the IUH of Storm 4) were used as starting values for the iteration procedure. After one iteration, the final run-off curve was found (Fig. 35). The predicted run-off hydrograph was almost identical with that obtained in Chapter 5 with Laguerre functions. Apparently the conceptual model chosen is highly suited to this quasilinear approach.

Summary

To predict run-off from intense rainfall in urban catchment areas, information is needed on critical sequences of rainfall amounts as well as a model for the transformation of rainfall into run-off.

Chapter 2 shows that, if a quarter of the lag time is taken as upper limit for the length of a sample interval, a sample interval of 15 s would be appropriate for rainfall and run-off modelling of two small paved inlet areas in the Netherlands. Gathering rainfall data with a time interval of 15 s seems however – apart from technical difficulties – not necessary. Rainfall is transformed into sewer inflow so fast in such paved inlet areas that it can be neglected in modelling run-off from parts of towns.

For urban catchment areas of 5×10^3 - 200×10^3 m^2, a sample interval of 1-2 min is needed. As this size seems an appropriate drainage unit for modelling urban run-off, it is recommended that rainfall be measured with a sample interval of 1 min. As especially short intense summer showers are critical for small urban catchment areas, data could be substantially reduced at the measuring site. Previous rainfall is of importance to determine losses. For this information, data with a much longer sample interval could be used. The appropriate interval should be determined during modelling and depends on the catchment and on the required accuracy.

Chapter 3 compared two methods of obtaining information about losses during transformation of rainfall into sewer inflow. Experiments with sprinklers on inlet areas are quicker and more reliable for this purpose than case studies on small urban catchment areas. Results are given of a study on transformation of rainfall into sewer inflow on a part of a flat roof. In this study, a rainfall simulator was used. The lag-and-route model (a time shift + a reservoir) proved suitable for this inlet area. In a study of paved inlet areas of a parking place in Wageningen and an asphalt road with a tiled footpath on both sides in Bennekom, the lag-and-route model again performed well. For the surface with concrete paving stones in Wageningen, infiltration rates were 7 - 27 mm/h, indicating high losses during transformation of rainfall into sewer inflow. Some simple loss models are described. An example is given showing that, in the process of modelling itself, a choice can be made between different loss models.

Chapter 4 discusses linearity and time invariance of catchment areas. Rainfall run-off systems are often represented by a series of two subsystems. The first subsystem represents losses in time and the second subsystem transforms net rainfall into run-off. In hydrology, it is usual to assume linear and time-invariant behaviour of the second subsystem. As a growing number of case studies point to non-linear behaviour of the second subsystem, two non-linear modelling approaches were distinguished. The quasilinear approach, which maintains linearity for each storm event but discriminates according to the magnitude of these events, proved the more practical approach. In tracer experiments, Pilgrim (1966, 1976) found evidence for quasilinearity. Two quasilinear methods are

described. The first one, which was suggested by Pilgrim and is supported by earlier investigations (Laurenson, 1964; Askew, 1970), uses the peak of run-off as criterion to choose an instantaneous unit hydrograph. In simulation problems, the peak of run-off is unknown beforehand, so this method requires iteration in application. The second quasi-linear method was successfully applied by Diskin (1973) for a catchment where Minshall (1960) demonstrated a marked non-linear behaviour. This method uses average rainfall as criterion to choose an instantaneous unit hydrograph. Both quasilinear methods were compared for a theoretical non-linear system, which consisted of a cascade of two equal non-linear reservoirs. This model belongs to a class of non-linear models which Dooge (1967b) proposed for catchment areas with non-linear behaviour. The method of Diskin (1973) gives problems for composite storms about where a continuous histogram of rainfall must be cut off to obtain separate events. The choice of these places greatly influences the results. Therefore a variant is proposed in which each bar of the rainfall histogram is convolution-integrated with an instantaneous unit hydrograph according to the average rainfall in a certain zone around that bar. The optimum length of this 'extent of influence' must be determined by trial and error.

Comparison of the two methods with the theoretical system showed that neither of the two methods yielded accurate outflow simulations. The variant of the method, as used by Diskin, had to be discarded as no indication was obtained about the length of the extent of influence. The method as suggested by Pilgrim (1976) yields better results than the linear approach. Therefore this method is selected for the Gray Haven catchment area, for which non-linear behaviour was demonstrated in Chapter 5.

The Gray Haven catchment, which lies about 11 km east of Baltimore, Maryland, United States, has a size of 0.094 km^2 and consists of a homogeneous residential area with 'group houses' on lots of about 250 m^2. Ground slopes are gentle (0.5%). As the pervious parts of the catchment (48% by area) are undergrass, the sod being underlain by sandy soil, these parts only seldom contribute significantly to sewer run-off. In the analysis, losses are treated by an initial loss (if necessary), followed by a proportional abstraction of the remaining losses. Nine storms were used for blackbox analysis with Laguerre functions. The shapes of the resulting instantaneous unit hydrographs indicated a marked non-linear behaviour. For the severe storms, high peaks and short times to peak were found.

Use of the quasilinear method as suggested by Pilgrim (1976) for the Gray Haven catchment area showed its feasibility. A run-off hydrograph of a composite storm was considerably better reconstructed by this method than by the linear approach. An alternative application of the quasilinear method was obtained if a conceptual model was used to identify the system instead of the general model with Laguerre functions. Chapter 6 compares six conceptual models for severe storms on the Gray Haven catchment area:

- the linear reservoir
- lag and route (a time shift + a linear reservoir)
- a cascade of a 'j model' and a linear reservoir
- the Nash cascade
- convective diffusion, upstream inflow
- convective diffusion, partial lateral inflow.

The Nash cascade and the convective diffusion models gave the best results. The test of the quasilinear method with the peak was repeated with convective diffusion, upstream inflow. Again the reconstructed outflow of a composite storm with the quasilinear method was considerably better than the linear reconstruction.

Samenvatting

Het in model brengen van stedelijke afvoer – een quasilineaire benadering

Om afvoeren ten gevolge van heftige neerslag te kunnen voorspellen is het noodzakelijk te beschikken zowel over informatie ten aanzien van kritieke opeenvolgingen van neerslaghoeveelheden als over een model dat de omzetting van neerslag in afvoer weergeeft.

In hoofdstuk 2 blijkt dat, indien de maximaal toelaatbare lengte voor het bemonsteringsinterval wordt gesteld op een kwart van de vertragingstijd, een bemonsteringsinterval van 15 s nodig zou zijn om twee kleine stroomgebiedjes van een straatkolk en een trottoirkolk in Nederland te beschrijven met een neerslag-afvoermodel. Het lijkt evenwel niet noodzakelijk om – nog afgezien van de technische problemen – neerslaggegevens te verzamelen met een tijdsinterval van 15 s. De omzetting van neerslag tot rioolinvoer verloopt bij dergelijke verharde stroomgebiedjes zo snel dat deze kan worden verwaarloosd bij het vervaardigen van modellen voor de afvoer uit stadsgedeelten.

Voor stedelijke stroomgebiedjes van $5 \times 10^3 \cdot 200 \times 10^3$ m^2 is een bemonsteringsinterval van 1-2 min vereist. Omdat deze oppervlakte geschikt lijkt voor het in model brengen van stedelijke afvoer, is het aan te bevelen neerslag te meten met een bemonsteringsinterval van 1 min. Omdat vooral korte hevige zomerse buien kritiek zijn voor kleine stedelijke gebieden zou er op de plaats waar wordt gemeten, reeds een aanzienlijke reductie van gegevens kunnen worden toegepast. Voorafgaande neerslag is van belang voor het bepalen van verliezen. Informatie hierover zou evenwel kunnen worden verkregen uit gegevens met een veel langer bemonsteringsinterval. De juiste lengte van dit interval zou tijdens het werken met modellen moeten worden vastgesteld en zal afhangen van het stroomgebied en de vereiste nauwkeurigheid.

In hoofdstuk 3 worden twee methoden om inzicht te krijgen in de verliezen die optreden gedurende de omzetting van neerslag in rioolinvoer, vergeleken. Er wordt vastgesteld dat voor dit doel sproeiproeven op stroomgebiedjes van kolken sneller en betrouwbaarder zijn dan studies van kleine stedelijke stroomgebiedjes.

Er worden resultaten gegeven van een studie over de omzetting van neerslag in rioolinvoer van een gedeelte van een plat dak. Voor deze studie is gebruik gemaakt van een beregeningsinstallatie. Het 'lag-and-route' model (een translatie + een reservoir) bleek een geschikt model te zijn voor deze 'inlet area'. Tijdens een studie van bestrate inlet areas op een parkeerterrein in Wageningen en een geasfalteerde straat met een betegeld trottoir aan weerskanten te Bennekom bleek het lag-and-route model wederom goed te voldoen. Voor de bestrating met betonstenen te Wageningen worden infiltratiesnelheden van 7 tot 27 mm/h gevonden, hetgeen betekent dat de omzetting van neerslag in rioolinvoer met grote verliezen gepaard kan gaan. Enkele eenvoudige modellen voor de beschrijving van verliezen worden beschreven. Met een voorbeeld wordt aangegeven hoe tijdens het werken met modellen een keuze kan worden gemaakt tussen verschillende modellen voor de beschrijving van verliezen.

In hoofdstuk 4 worden lineariteit en tijdsinvariantie van stroomgebieden besproken. Neerslag-afvoersystemen worden dikwijls weergegeven door middel van twee in serie geschakelde subsystemen. Het eerste subsysteem geeft het verloop van de verliezen in de tijd weer, terwijl het tweede subsysteem de omzetting van netto neerslag in afvoer beschrijft. Het is in de hydrologie gebruikelijk lineair en tijdsinvariant gedrag aan te nemen van het tweede subsysteem. Daar een groeiend aantal onderzoekingen van stroomgebieden uitwijst dat het tweede subsysteem niet lineair reageert, is een indeling gemaakt in twee benaderingswijzen, waarbij niet-lineaire modellen worden gehanteerd. Er wordt vastgesteld dat de quasilineaire benadering, waarbij lineariteit wordt verondersteld tijdens een neerslaggebeurtenis, maar waarbij onderscheid wordt gemaakt al naar gelang de zwaarte van gebeurtenissen, het meest praktisch lijkt.

Resultaten van proefnemingen met tracers door Pilgrim (1966, 1976) ondersteunen de opvatting van quasi-lineariteit. Er worden twee quasilineaire methoden beschreven. De eerste, welke was voorgesteld door Pilgrim en die wordt geschraagd door eerdere onderzoekingen (Laurenson, 1964; Askew, 1970), gebruikt de afvoerpiek als criterium voor de keuze van een ogenblikkelijke eenheidsafvoergolf (IUH). Omdat bij simulatievraagstukken de afvoerpiek vooraf onbekend is, moet bij toepassingen van deze methode iteratief worden gewerkt. De tweede quasilineaire methode werd door Diskin (1973) met succes toegepast op een stroomgebied waarvan Minshall (1960) een uitgesproken niet-lineair gedrag had aangetoond. Deze methode werkt met de gemiddelde neerslagintensiteit als criterium voor de keuze van een ogenblikkelijke eenheidsafvoergolf. Beide quasilineaire methoden worden vergeleken met behulp van een theoretisch niet-lineair systeem dat bestaat uit een serie van twee gelijke niet-lineaire reservoirs. Dit model behoort tot de klasse niet-lineaire modellen die Dooge (1967b) voorstelt te gebruiken, indien men te maken heeft met stroomgebieden met een niet-lineair gedrag. De methode van Diskin (1973) levert moeilijkheden op bij samengestelde neerslaggebeurtenissen voor wat betreft de plaatsen waar in een doorlopend neerslaghistogram moet worden geknipt om afzonderlijke gebeurtenissen te verkrijgen. De keuze van deze plaatsen heeft een belangrijke invloed op het resultaat. Daarom wordt een variant voorgesteld waarbij voor ieder staafje van het neerslaghistogram de convolutie-integraal wordt berekend met een ogenblikkelijke eenheidsafvoergolf (IUH) welke wordt gekozen volgens de gemiddelde neerslagintensiteit gedurende een zekere tijd voor en na het beschouwde staafje. De optimale lengte van deze 'invloedsfeer' moet proberend worden vastgesteld.

Bij vergelijking van de twee methoden aan de hand van het theoretische systeem leverde geen van de methoden accurate afvoersimulaties. De variant van de methode van Diskin moest terzijde worden geschoven, daar geen criterium werd gevonden voor de te kiezen lengte van de invloedsfeer. De methode die Pilgrim (1976) voorstelde, gaf betere resultaten dan de lineaire benadering. Daarom is deze methode gekozen voor een toepassing op het stroomgebied Gray Haven, waarover het niet-lineaire gedrag wordt aangetoond in hoofdstuk 5.

Het stroomgebied Gray Haven, dat ongeveer 11 km ten oosten van Baltimore (Maryland, Verenigde Staten) is gelegen, beslaat een oppervlak van 0.094 km^2 en bestaat uit een homogeen opgebouwde woonwijk met een perceelsgrootte van 250 m^2. De helling van het terrein bedraagt gemiddeld 0.5%. Daar de doorlatende delen van het stroomgebied (48% van de totale oppervlakte) begroeid zijn met gras en bestaan uit zandige grond,

dragen deze slechts zelden bij tot de rioolafvoer. In de analyse zijn de verliezen in model gebracht door een initieel verlies (indien noodzakelijk), gevolgd door een proportionele verrekening van het resterende verlies. Voor negen buien is een 'blackbox' analyse met Laguerre functies uitgevoerd. De vormen van de aldus verkregen ogenblikkelijke eenheidsafvoergolven wijzen op een uitgesproken niet-lineair gedrag. Voor de hevige buien werden hoge pieken en lage waarden voor de tijd tot het optreden van de piek gevonden.

Toepassing van de quasilineaire methode, zoals geopperd door Pilgrim (1976), op het stroomgebied van Gray Haven toont de toepasbaarheid van deze methode aan. Het afvoerverloop ten gevolge van een samengestelde bui werd met deze methode aanzienlijk beter gereconstrueerd dan met de lineaire benadering.

Een alternatieve toepassing van de quasilineaire methode bestaat hieruit dat een zogenaamd 'conceptual model' wordt toegepast om het systeem te identificeren in plaats van het algemene model met Laguerre functies. In hoofdstuk 6 worden zes 'conceptual models' voor het stroomgebied Gray Haven vergeleken aan de hand van enkele zware buien, te weten:

- het lineaire reservoir
- 'lag-and-route' (een translatie + een lineair reservoir)
- een '*j* model' en een lineair reservoir in serie
- de Nash cascade
- convectieve diffusie, bovenstroomse invoer
- convectieve diffusie, gedeeltelijke zijdelingse invoer.

De Nash cascade en de convectieve-diffusiemodellen leverden het beste resultaat. De test van de quasilineaire methode die gebruik maakt van de afvoerpiek, is herhaald met toepassing van het model, convectieve diffusie, bovenstroomse invoer. Het met de quasilineaire methode gereconstrueerde afvoerverloop van een samengestelde bui is wederom aanzienlijk beter dan dat van de lineaire benadering.

References

Abramowitz, M. & I.A. Stegun, 1965. Handbook of mathematical functions. Dover publications Inc., New York.

Amorocho, J. & G.T. Orlob, 1961. Nonlinear analysis of hydrologic systems. Water Resources Center contribution 40, University of California, Berkeley.

Ardis, C.V. et al., 1969. Storm drainage practices of thirty-two cities. J. Hydraul. Div. Am. Soc. Div. Eng. (HY 1): 383-408.

Askew, A.J., 1970. Variation in lag time for natural catchments. J. Hydraul. Div. Am. Soc. Civ. Eng. (HY 2): 317-330.

Childs, E.F., 1958. Northeastern floods of 1955; Flood control hydrology. Proceedings paper 1663. J. Hydraul. Div. Am. Soc. Div. Eng. 84 (HY 3).

Cole, J.A. & J.D.F. Sherriff, 1972. Some single- and multi-site models of rainfall within discrete time increments. J. Hydrol. 17: 97-113.

Delleur, J.W. & A.R. Rao, 1973. Some extensions of linear systems analysis in hydrology. Proceedings of the Second International Symposium in Hydrology, Fort Collins, Colorado. p. 117-132.

Diskin, M.H., 1973. The role of lag in a quasi-linear analysis of the surface runoff system. Proceedings of the Second International Symposium in Hydrology, Fort Collins, Colorado. p. 133-144.

Diskin, M.H. & A. Boneh, 1972. Properties of the kernels for time invariant, initially relaxed, second order, surface runoff systems. J. Hydrol. 17: 115-141.

Dommerholt, A. & J.G. Zondervan, 1977. De toevoer van regenwater naar een straatkolk. H_2O 10: 204-207.

Dooge, J.C.I., 1965. Analysis of linear systems by means of Laguerre functions. Soc. Ind. Appl. Math., J. Control, Ser. A,2(3): 396-408. Philadelphia.

Dooge, J.C.I., 1967a. Hydrologic systems with uniform non-linearity. Memorandus University College, Civil Engineering Department, Cork.

Dooge, J.C.I., 1967b. A new approach to nonlinear problems in surface water hydrology. International Association of Scientific Hydrology. General Assembly of Bern.

Dooge, J.C.I., 1974. Problems and methods of rainfall-runoff modelling. Workshop on Mathematical Models in Hydrology. University of Pavia, Institute of Hydraulics.

Garvey, B.J., 1972. The analysis of linear systems by means of Laguerre and Meixner functions. Thesis National University of Ireland, Dublin.

Gastel, J.M. van, 1976. Een vergelijkend hydrologisch modelonderzoek. Essay Agricultural University of Wageningen, Department of Hydraulics and Catchment Hydrology.

Grace, R.A. & P.S. Eagleson, 1966. The synthesis of short-time-increment rainfall sequences. Massachusetts Institute of Technology, Department of Civil Engineering, Hydrodynamics Laboratory report No. 91.

Harley, B.M. et al., 1970. A modular distributed model of catchment dynamics. Massachusetts Institute of Technology, Department of Civil Engineering, Hydrodynamics Laboratory technical report No. 133.

Hayami, S., 1951. On the propagation of floodwaves. Disaster Prev. Res. Inst., Kyoto Univ., Bull. 1.

Kloet, P. van der et al., 1977. Calculation of instantaneous unit hydrographs in an urban area. International Symposium on the effects of urbanization and industrialization on the hydrological regime and on water quality. Amsterdam. p. 124-143.

KNMI, 1968. Detailanalyse van Pluviogrammen A. KNMI, De Bilt.

Koninklijk Instituut van Ingenieurs, 1972. Rapport van de commissie riolering en waterverontreiniging van de afdeling voor gezondheidstechniek. H_2O 5: 199-260.

Kraijenhoff van de Leur, D.A., 1958. A study of non-steady groundwater flow with special reference to a reservoir coefficient. De Ingenieur, B, 70 (19): 87-94.
Laurenson, E.M., 1964. A catchment storage model for runoff routing. J. Hydrol. 2: 141-163.
McPherson, M.B., 1969. Some notes on the rational method of storm drain design. ASCE Urban Water Resources Research Program. Technical Memorandum No. 6.
McPherson, M.B. 1974. Problems in modeling urban watersheds. Water Resour. Res., 10 (3): 434-440.
McPherson, M.B., 1976. Urban water resources. Water Resour. Res. 57 (11): 798-806.
Minshall, N.E., 1960. Predicting storm runoff on small experimental watersheds. J. Hydraul. Div. Am. Soc. Civ. Eng. 86 (HY 8): 17-38.
Nash, J.W. 1959. Systematic determination of unit hydrograph parameters. J. Geophys. Res. 64 (1): 111-115.
National Environment Research Counsel, 1975. Flood Studies Report. 27 Charing Cross road, London.
Nes, T.J. van de, 1973. Linear analysis of a physically based model of a distributed surface runoff system. Thesis Landbouwhogeschool, Wageningen.
Pilgrim, D.H., 1966. Radioactive tracing of storm runoff on a small catchment. 2. Discussion of results. J. Hydrol. 4: 306-326.
Pilgrim, D.H., 1976. Travel times and nonlinearity of flood runoff from tracer measurements on a small watershed. Water Resour. Res. 12 (3): 487-496.
Raudkivi, A.J. & N. Lawgun, 1970. A markov chain for rainfall generation IASH Symposium of research on representative and experimental basins, Wellington, New Zealand. Publ. No. 96. p. 269-278.
Sarma, P.B.S. et al., 1973. Comparison of rainfall-runoff models for urban areas. J. hydrol. 18 1-19.
Schaake jr, J.C. et al., 1967. Experimental examination of the rational method. J. Hydraul. Div. Am. Soc. Civ. Eng. (HY 6): 353-370.
Schenkeveld, M.M., 1976. Regengegevens uit de 5-minuten analyse. Engineering company Dwars, Heederik en Verhey, Amersfoort.
Schönfeld, J.C., 1948. Voortplanting en verzwakking van hoogwatergolven op een rivier. De Ingenieur, B., jan: 1-7.
Singh, K.P., 1964. Nonlinear instantaneous unit-hydrograph theory. J. Hydraul. Div. Am. Soc. Div. Eng. (HY 2): 313-347.
Tholin, A.L. & C.J. Keifer, 1960. Hydrology of urban run-off. Trans. Am. Soc. Civ. Eng. 125: 1308-1355.
Tucker, L.S., 1969. Availability of rainfall-runoff data for sewered catchments. ASCE Urban Water Resources Research Program. Technical Memorandum No 8.
Viessman jr, W., 1966. The hydrology of small impervious areas. Water Resour. Res. 2 (3): 405-412.
Watkins, L.H., 1963. Research on surface-water drainage. Proc. Inst. Civ. Eng. paper No 6638.
Yperlaan, G.J., 1977. Statistical evidence of the influence of urbanization on precipitation in the Rijnmond area. International Symposium on the effects of urbanization and industrialization on the hydrological regime and on water quality. Amsterdam.
Zondervan, J.G. & A. Dommerholt, 1975. Omvorming van neerslag tot rioolinvoer bij één bepaald type 'inlet area'. Nota 33, Department of hydraulics and catchment hydrology. Landbouwhogeschool, Wageningen.
Zondervan, J.G. & A. Dommerholt, 1976. Omvorming van neerslag tot rioolinvoer bij enkele typen verhardingen. Nota 38, Department of hydraulics and catchment hydrology. Landbouwhogeschool, Wageningen.

List of symbols

		dimension
a, b, c	coefficients	
α, β, γ	coefficients in Laguerre expansions	
A_τ	translation coefficient	L/T
$\Gamma(\nu)$	gamma function	
D	diffusion coefficient	L^2/T
$\Phi_n(t)$	ordinary n^{th} Laguerre function	
G	parameter, m/l	
$h(t)$	instantaneous unit hydrograph	1/T
H	dimensionless length parameter, $l \cdot A_\tau / 2D$	
I	characteristic time parameter, $2D/A_\tau^2$	T
j	reservoir coefficient of the 'j model'	T
k	lag time of a linear reservoir	T
l	length of a channel section	L
$L_n(t)$	ordinary Laguerre polynominal of degree n	
m	length over which lateral inflow takes place	
ν	parameter indicating the number of linear reservoires in a Nash cascade	
$p(t)$	input	L/T or L^3/T
$\bar{p}$	average input	L/T or L^3/T
P_i	bar of input histogram	L or L^3
$q(t)$	outflow, run-off rate	L/T or L^3/T
q_p	peak of outflow, peak run-off rate	L/T or L^3/T
r_i	criterion to choose IUH	
R_t	section of time coordinate	T
S	storage volume	L^3
S^*	dimensionless storage volume	
S_e	a unit of storage volume	L^3
t	time coordinate	T
t^*	dimensionless time	
t_p	time to peak of IUH	T
t_e	a unit of time	T
T	duration of input	T
Δt	time interval	T
τ	time shift	T
t_l	lag time of the instantaneous unit hydrograph	T
U_p	peak of the instantaneous unit hydrograph	1/T
x	length coordinate	L
Z	time-scale factor	

Appendix 1

Determination of IUH by means of Laguerre functions

This appendix deals with the determination of a non-parametric IUH, using ordinary Laguerre functions. Application of Laguerre functions in hydrology was introduced by Dooge (1965). Garvey (1972) gave some results of this application.

Ordinary Laguerre functions may be defined by

$$\Phi_n(t) = e^{-t/2} L_n(t) \quad , \quad n = 0,1,2,... \tag{A1.1}$$

where $L_n(t)$ is the ordinary Laguerre polynomial of degree n:

$$L_n(t) = \sum_{m=0}^{m=n} (-1)^n \binom{n}{m} \frac{t^m}{m!} \tag{A1.2}$$

The set of Laguerre functions is complete with respect to the range $[0,\infty]$, i.e. any sectionally continuous function $f(t)$, defined for $t \geqslant 0$, may be expanded into an infinite series of Laguerre functions. Moreover these functions are orthonormal:

$$\int_0^\infty \Phi_m(t)\, \Phi_n(t) \mathrm{d}t = \delta_{mn} \tag{A1.3}$$

with $m,n = 0,1,2,...$

δ_{mn}: kronecker delta.

In virtue of the orthonormality property (Eq. A1.3), the coefficients α_n in the expansion

$$f(t) = \sum_{n=0}^{n=\infty} \alpha_n \Phi_n(t) \tag{A1.4}$$

are given by

$$\alpha_n = \int_0^\infty f(t)\, \Phi_n(t) \mathrm{d}t \tag{A1.5}$$

Expanding $f(t)$ into a finite series of Laguerre functions, a best approximation in the sense of least squares is obtained if α_n is given by Equation A1.5.

Input, output and IUH are expanded into a series of Laguerre functions,

$$p(t) = \sum_{n=0}^{n=\infty} \alpha_n \Phi_n(t) \ , \tag{A1.6a}$$

$$q(t) = \sum_{n=0}^{n=\infty} \beta_n \Phi_n(t) \ , \qquad \text{(A1.6b)}$$

$$h(t) = \sum_{n=0}^{n=\infty} \gamma_n \Phi_n(t) \ . \qquad \text{(A1.6c)}$$

If $p(t)$ and $q(t)$ are certain functions for $t \geqslant 0$, the coefficients α_n and β_n can be obtained from

$$\alpha_n = \int_0^{\infty} p(t) \Phi_n(t) \mathrm{d}t \qquad \text{(A1.7a)}$$

$$\beta_n = \int_0^{\infty} q(t) \Phi_n(t) \mathrm{d}t \qquad \text{(A1.7b)}$$

In the identification problem, $h(t)$ is unknown, hence the coefficients γ_n are unknown. These can be evaluated by substituting the expansions (Eq. A1.6a and A1.6b) in the convolution-integral

$$q(t) = \int_0^t h(t-\tau) p(\tau) \mathrm{d}\tau \qquad \text{(A1.8)}$$

In this way the following relations between α_n, β_n and γ_n are obtained (Dooge, 1965)

$$\beta_k = \sum_{n=0}^{n=k} \gamma_n \alpha_{k-n} - \sum_{n=0}^{n=k-1} \gamma_n \alpha_{k-n-1} \ , \qquad \text{(A1.9)}$$

with $k = 0,1,...$

Defining

$$\beta_k^* = \sum_{i=0}^{i=k} \beta_i \ , \qquad \text{(A1.10)}$$

the Equations A1.9 may be simplified to

$$\beta_k^* = \sum_{n=0}^{n=k} \gamma_n \alpha_{k-n} \ , \qquad \text{(A1.11)}$$

with $k = 0,1,...$
The unknown coefficients γ_n are determined by solving the linear equations A1.11. Then $h(t)$ is given by Equation A1.6c.

Practical aspects

In practical applications of the foregoing, the following problems must be solved:
– sectionally continuous functions $p(t)$ and $q(t)$ must be constructed from records of

effective precipitation and run-off and the integrals in Equation A1.7 must be evaluated;
- a unit of time (time-scale factor) must be chosen;
- only a finite series of Laguerre functions can be used;
- the set of Equations A1.11 must be solved.

The record of effective precipitation consists of volumes of rainfall in successive time intervals R_i, with

$$R_i = \{t, t_{i-1} < t \leqslant t_i\} \ , \ i = 1,2,...N \tag{A1.12}$$

which usually all have the same value Δt. Input integrated over the time interval R_i is denoted by P_i. A function $p(t)$ is constructed assuming that $p(t)$ is constant in each interval:

$$p(t) = \frac{P_i}{\Delta t} \ , \ t \in R_i \tag{A1.13}$$

Since the run-off is given at the discrete times t_i, $i = 0,1, ...$, it is assumed that the run-off is linear in each interval R_i,

$$q(t) = q_{i-1} + (q_i - q_{i-1}) \ (\frac{t-t_{i-1}}{\Delta t}) \ , \ t \in R_i \tag{A1.14}$$

where $q_i = q(t_i) \ , \ i = 0,1,...$

The integrals in the right side of Equation A1.7 are evaluated numerically by applying the trapezoidal rule to sufficiently small intervals. The functions $\Phi_n(t)$ are computed by means of the following recurrence relationship:

$$(n + 1) \Phi_{n+1}(t) = (2n + 1-t) \Phi_n(t) - n \Phi_{n-1}(t) \tag{A1.15}$$

In the preceding section, it is assumed that t is a dimensionless (time) coordinate. Hence a unit of time Z (time-scale factor) has to be selected and expressed in the sample time Δt. The choice of the factor affects the form of the input and output and consequently the coefficients in the expansions (Eq. A1.6). In addition, the accuracy of the result depends on the time-scale factor for any fixed number of Laguerre functions N. In order to select a suitable value of Z,

$$\int_0^\infty h(t)\mathrm{d}t = 2 \sum_{m=0}^{m=N} (-1)^m \gamma_m \tag{A1.16}$$

is computed for $Z = \Delta t$, $2\Delta t$, $4\Delta t$ and $8\Delta t$ and that value of Z is selected, that gives a satisfactory description of input and output, yields a value for the integral in Equation A1.16 that is close to 1.0 and gives an IUH without or with hardly any oscillation. Of course also the choice of the number of Laguerre functions used in the expansions (Eq. A1.6) is of importance. For less complicated storms, 20 functions appeared to give a sufficiently accurate approximation of input and output, provided that a suitable time-scale factor was used.

By halving the integration interval, it was found that for 20 Laguerre functions the numerical integration of these functions was sufficiently accurate if one time unit was divided into 8 equal intervals. Using this integration interval means that, for $Z = \Delta t$, the integration interval coincides with $\Delta t/8$ and that for $Z = 8\Delta t$ the integration interval coincides with Δt.

Each time the identification process was carried out, the set of linear Equations A1.11 had to be computed. This may be achieved by means of successive substitution as follows: the first equation yields a value of γ_0, substituting this value into the second equation a value of γ_1 is obtained, etc.

However the solution obtained in this way is sensitive to disturbances in α_n and β_n and is therefore less suitable. For that reason more equations are established than the number of unknowns γ_n and the method of least squares is applied in order to compute γ_n. Writing the set of equations in matrix notation,

$$AC = B \tag{A1.17}$$

where A is a coefficient matrix, C the vector of unknowns and B the vector with components β_k*, the solution reads

$$C = (A^{\mathrm{T}}A)^{-1}A^{\mathrm{T}}B \tag{A1.18}$$

In running the computer program, the number of Laguerre functions for description of IUH was varied, as the optimum number was unknown beforehand.

Appendix 2

A cascade of non-linear reservoirs

For a cascade of equal non-linear reservoirs, the outflow $q_i(t)$ from Reservoir i is related to the storage $S_i(t)$ in that reservoir by the equation

$$q_i(t) = a \cdot S_i^c(t) \tag{A2.1}$$

where a,c are coefficients. The equation of continuity for that reservoir reads

$$\frac{dS_i(t)}{dt} = q_{i-1}(t) - q_i(t) \tag{A2.2}$$

From Equations A2.1 and A2.2,

$$\frac{dS_i(t)}{dt} + a \cdot S_i^c(t) = q_{i-1}(t) \tag{A2.3}$$

So a cascade of n reservoirs can be represented by the following set of equations:

$$\begin{aligned}
&\frac{dS_1(t)}{dt} + a \cdot S_1^c(t) = p(t) \\
&\frac{dS_2(t)}{dt} + a \cdot S_2^c(t) = a \cdot S_1^c(t) \\
&\vdots \qquad\qquad \vdots \qquad\qquad \vdots \\
&\frac{dS_i(t)}{dt} + a \cdot S_i^c(t) = a \cdot S_{i-1}^c(t) \\
&\vdots \qquad\qquad \vdots \qquad\qquad \vdots \\
&\frac{dS_n(t)}{dt} + a \cdot S_n^c(t) = a \cdot S_{n-1}^c(t)
\end{aligned} \tag{A2.4}$$

with $p(t)$ as inflow into the first reservoirs.

By introducing a unit of time t_Θ and a unit of storage S_Θ, Equation A2.4 can be transformed into dimensionless form.

Set $t = t^* t_\Theta$ and $S = S^* S_\Theta$, then t^* and S^* are dimensionless variables.

Substitution in Equation A2.4 yields:

$$\frac{S_\Theta dS_1^*}{t_\Theta dt^*} + a \cdot S_\Theta^c \cdot S_1^{*c} = p(t_\Theta t^*)$$

or

$$\left.\begin{aligned}
&\frac{dS_1^*(t^*)}{dt^*} + a_\ominus \cdot S_1^{c*}(t^*) = z(t^*) \\
&\text{where } a_\ominus \text{ is } a \cdot t_\ominus \cdot S_\ominus^{c-1} \text{ and } z(t^*) \text{ is } (t_\ominus/S_\ominus)p(t_\ominus t^*), \text{ both dimensionless.} \\
&\frac{dS_2^*(t^*)}{dt^*} + a_\ominus \cdot S_2^{c*}(t^*) = a_\ominus \cdot S_1^{c*}(t^*) \\
&\quad\vdots \qquad\qquad \vdots \qquad\qquad \vdots \\
&\frac{dS_i^*(t^*)}{dt^*} + a_\ominus \cdot S_i^{c*}(t^*) = a_\ominus \cdot S_{i-1}^{c*}(t^*) \\
&\quad\vdots \qquad\qquad \vdots \qquad\qquad \vdots \\
&\frac{dS_n^*(t^*)}{dt^*} + a_\ominus \cdot S_n^{c*}(t^*) = a_\ominus \cdot S_{n-1}^{c*}(t^*)
\end{aligned}\right\} \quad \text{(A2.5)}$$

The corresponding dimensionless outflow from Reservoir i is:

$$q_i^*(t^*) = (t_\ominus/S_\ominus)q_i(t_\ominus t^*),$$

which combined with Equation A2.1 yields

$$q_i^*(t^*) = a \cdot t_\ominus \cdot S_\ominus^{c-1} \cdot S_i^{c*}(t^*) = a_\ominus \cdot S_i^{c*}(t^*) \quad \text{(A2.6)}$$

Question. If for a certain inflow into the cascade $p_1(t)$ the outflow $q_1(t)$ is known, does there then exist a class of inflows $p_2(t)$ for which the corresponding outflows $q_2(t)$ can directly be derived?

This will be so as long as the same dimensionless Equations A2.5 can be obtained in both cases. This implies that $a_\ominus$ and $z(t^*)$ must not change. If inflow rates $p_1(t)$ and $p_2(t)$ are expressed in time units t_1 and t_2, respectively, and the corresponding storage S in unit volumes S_1 and S_2, then in Equation A2.5

$$a \cdot t_1 \cdot S_1^{c-1} = a_\ominus = a \cdot t_2 \cdot S_2^{c-1} \quad \text{(A2.7)}$$

and

$$\frac{t_1 \cdot p_1(t_1 t^*)}{S_1} = z(t^*) = \frac{t_2 \cdot p_2(t_2 t^*)}{S_2} \quad \text{(A2.8)}$$

From Equation A2.7, it follows that

$$S_2^{c-1} = \frac{t_1}{t_2} S_1^{c-1}$$

$$S_2 = S_1 \left(\frac{t_1}{t_2}\right)^{\frac{1}{c-1}} \quad \text{(A2.9)}$$

Substitution of Equation A2.9 in A2.8 yields:

$$p_2(t_2 \cdot t^*) = (\frac{t_1}{t_2})^{\frac{c}{c-1}} \; p_1(t_1 \cdot t^*) \tag{A2.10}$$

Conclusion. The same dimensionless Equations A2.5 are obtained if, for inflow rates p_2, which differ by a factor $\eta = (t_1/t_2)^{c/(c-1)}$ from p_1, the time scale is adjusted according to Equation A2.10.

Let q_{i_1} denote the outflow from Reservoir i for the inflow p_1, and q_{i_2} the outflow from Reservoir i for the inflow p_2, then for the corresponding dimensionless outflows

$$q_i^*(t^*) = \frac{t_1 \cdot q_{i_1}(t_1 t^*)}{S_1} = \frac{t_2 \cdot q_{i_2}(t_2 t^*)}{S_2} \tag{A2.11}$$

$$q_{i_2}(t_2 \cdot t^*) = \frac{S_2 \cdot t_1}{S_1 \cdot t_2} \quad q_{i_1}(t_1 \cdot t^*) \tag{A2.12}$$

Substitution of Equation A2.9 in A2.12 yields

$$q_{i_2}(t_2 \cdot t^*) = (\frac{t_1}{t_2})^{\frac{c}{c-1}} \; q_{i_1}(t_1 \cdot t^*)$$

so

$$q_{i_2}(t_2 \cdot t^*) = \eta \cdot q_{i_1}(t_1 \cdot t^*) \tag{A2.13}$$

Conclusion. If $p_2(t)$ equals a factor η times $p_1(t)$, the outflow from the cascade $q_{n_2}(t)$ can be obtained as $\eta \cdot q_{n_1}(t)$, after rescaling this curve.

As $\eta = (t_1/t_2)^{c/(c-1)}$, it follows that $t_2 = \eta^{-(c-1)/c} t_1$

Appendix 3

Comparison of two quasilinear methods with a theoretical model

To compare the quasilinear methods as described in Chapter 4, a theoretical non-linear model was used. To this end, a cascade of two equal non-linear reservoirs was chosen, with arbitrary units of time and length. For one reservoir,

$$q = a \cdot S^c \tag{A3.1}$$

where q is run-off, S is storage volume and a,c coefficients. The continuity equation reads

$$p - q = \frac{dS}{dt} \tag{A3.2}$$

where p is inflow. As $p\text{-}q = dS/dt = (dS/dq)(dq/dt) = (1/a)^{1/c}(1/c)\, q^{(c-1)/c}(dq/dt)$, one obtains

$$\frac{dq}{dt} = \frac{p-q}{\left(\frac{1}{a}\right)^{1/c} \frac{1}{c} q^{(c-1)/c}} \tag{A3.3}$$

For the coefficients, a 0.3 and c 1.5 was chosen. For some inflow patterns p, outflow was calculated by solving Equation A3.3 with the method of Runge-Kutta for the first and second reservoir, respectively.

First the effect of the duration of inflow T on the resulting IUH was investigated by linear identification as described in Appendix 1. As inflow, p 1.0 was chosen. Identification was carried out for inflow durations T = 1, 2, 4, 8 and 16, respectively. Some results of the identifications are given in Table A3.1.

Table A3.1. Identification results for block-shaped inflows with intensity p 1 and different durations of inflow, T. Time-scale factor $Z = \Delta t/2$; 20 Laguerre functions are used to approximate the inflow and outflow.

T	Peak of outflow q_p	$\int_0^\infty h(t) \cdot dt$	Number of Laguerre functions for $h(t)$
1	0.076	0.99	11
2	0.213	1.01	9
4	0.544	1.01	6
8	0.930	1.00	6
16	0.999	1.01	5

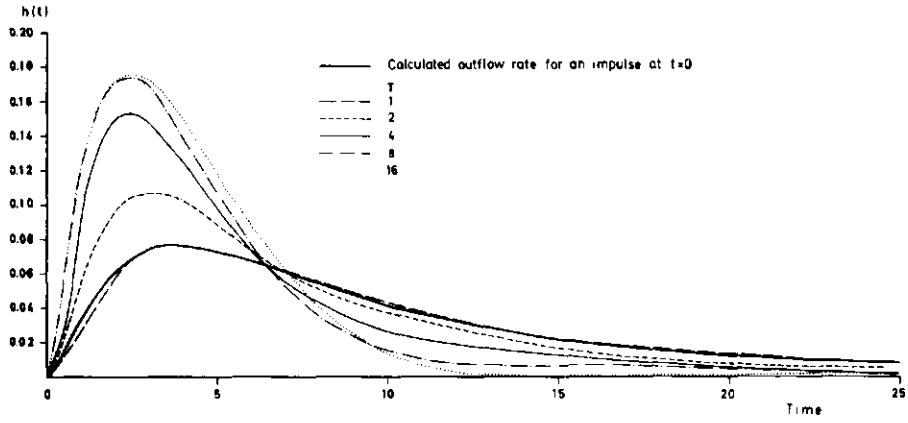

Fig. A3.1. Instantaneous unit hydrographs, $h(t)$, for p 1 and T variable.

Resulting IUH is given in Figure A3.1, together with the outflow for an impulse at t 0, which was obtained by numerical solution of Equation A3.3 with the initial condition q = a for the first reservoir, q = 0 for the second reservoir. Figure A3.1 shows that the IUH for T 1 hardly differs from the calculated outflow for an impulse input at t 0. For $T > 1$, IUH shows higher peaks for greater values of T. For $T \geqslant 8$, the form of the IUH changes very little. For $T \geqslant 8$, the peak of outflow q_p approaches the inflow.

To get some insight into the accuracy of applying linear identification to this non-linear model, the five outflows are reconstructed by convolution-integrating the five

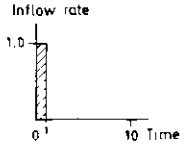

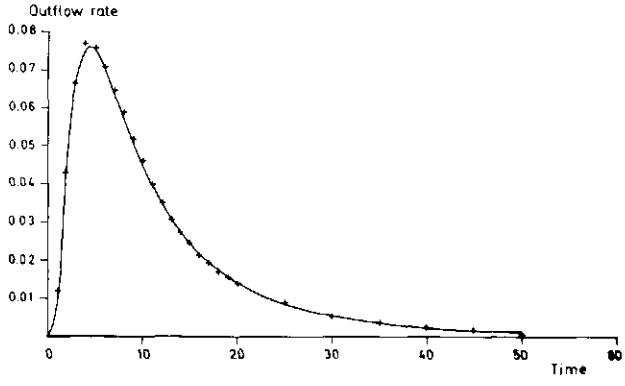

Fig. A3.2. Linear reconstruction of outflow for T 1. — calculated outflow, ++ reconstructed outflow.

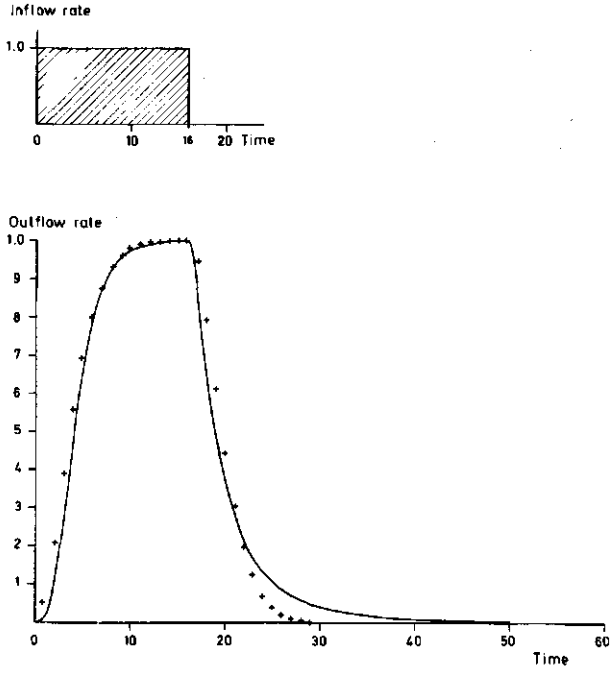

Fig. A3.3. Linear reconstruction of outflow for T 16. — calculated outflow, ++ reconstructed outflow.

inflows with their corresponding IUH. Figure A3.2 and A3.3 compare numerically computed outflows with linear reconstructions of outflow waves for T 1 and T 16. For p 1 and T 1, an excellent reconstruction is found, whereas for p 1 and T 16 the reconstructed outflow differs considerably from the calculated outflow. For T 16 the falling limb of the hydrograph shows a particularly poor agreement.

Thereupon the effect of the value of block-shaped inflows on the resulting IUH was investigated for two durations of inflow, T 16 and T 3. According to Appendix 2, inflows with the same duration T and different p cannot be considered as similar inflows in the sense of uniform non-linearity. The value T 16 was chosen because for this duration of inflow, IUH reaches its highest peak, because of approximation to steady state during inflow. The value T 3 was chosen to identify the model also for a duration of inflow shorter than the length of the four segments of a 'test storm' presented below.

The resulting IUH for inflow p 1, 4, 8, 12 and 16 for T 16 and p 1, 2, 4, 8 and 16 for T 3 are given in Figure A3.4A and A3.4B. Some results of the identifications are given in Table A3.2 Table A3.2 shows that, for both T 16 and T 3, the product of the time to peak t_p and the peak U_p yielded approximately the same value for the five IUH. This suggests that the five IUH may have the same basic shape. To investigate this, for both T 16 and T 3 the IUH for p 1, 4 and 16 are reduced to the basic shape (Fig. A3.5A and A3.5B). For both T 16 and T 3, the three reduced IUH approximately coincide. Figure A3.6 shows for T 3 the outflows from the block-shaped inflows with p 1, 4 and 16 in the dimensionless shape. This figure shows that these shapes are different.

For different values of T, the product $t_p \cdot U_p$ of the IUH will vary (e.g. Table A3.2). For a given value of p, the product $t_p \cdot U_p$ 0.45, as found for T 16, will be the highest value, because the shape of the IUH will not vary any more for greater duration T.

For the calculated outflow from an impulse at t 0 (Fig. A3.1) $t_p \cdot U_p = 0.29$, so if the identifications of Figure A3.4 be repeated for other values of T, the product $t_p \cdot U_p$ would vary between 0.29 and 0.45.

To allow comparison of quasilinear methods, it was decided to use IUH for the value T 16, which is the duration of inflow that yields IUH with the highest value of $U_p \cdot t_p$.

In the following comparison, a basic shape of IUH was not yet used. Instead the IUH for p 1, 4 and 16 (Fig. A3.4A) were used.

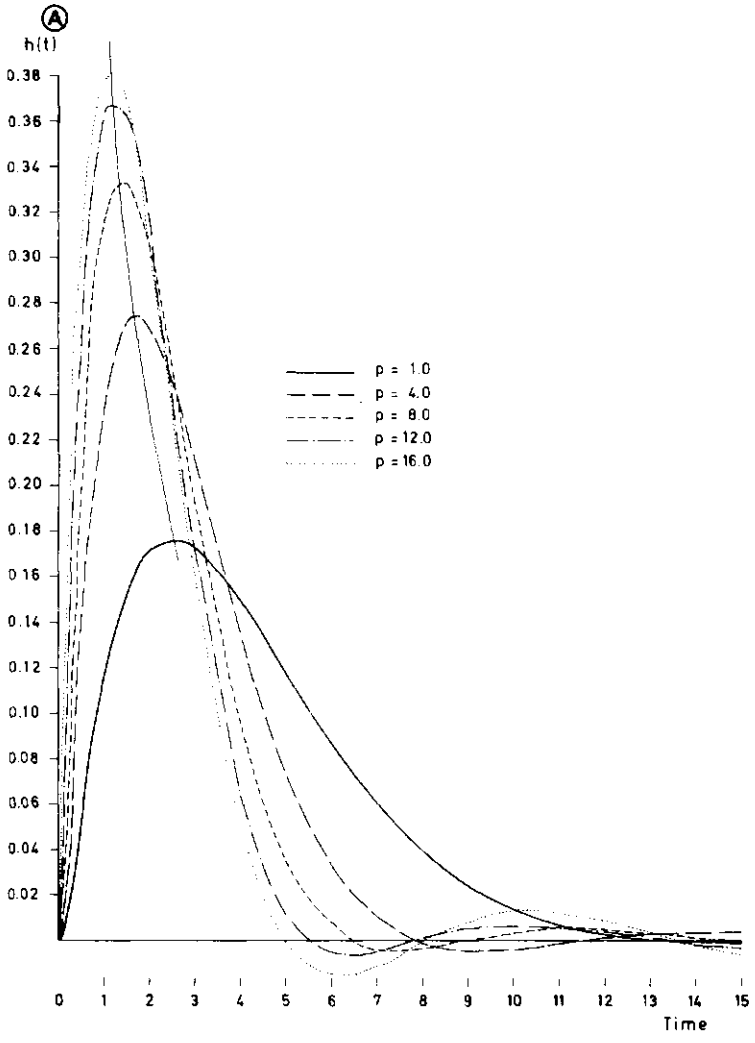

Experiment with average input as criterion

Apart from the three IUH for p 1, 4 and 16 a relation between average inflow, $\overline{p}$, and the peak of the IUH, U_p, is needed, to select for every bar of the input histogram the appropriate IUH. This relation is established with the five IUH from Figure A3.4A and is given in Fig. A3.7.

In the experiment, the average input $\overline{p}$ over a certain length of time around every bar

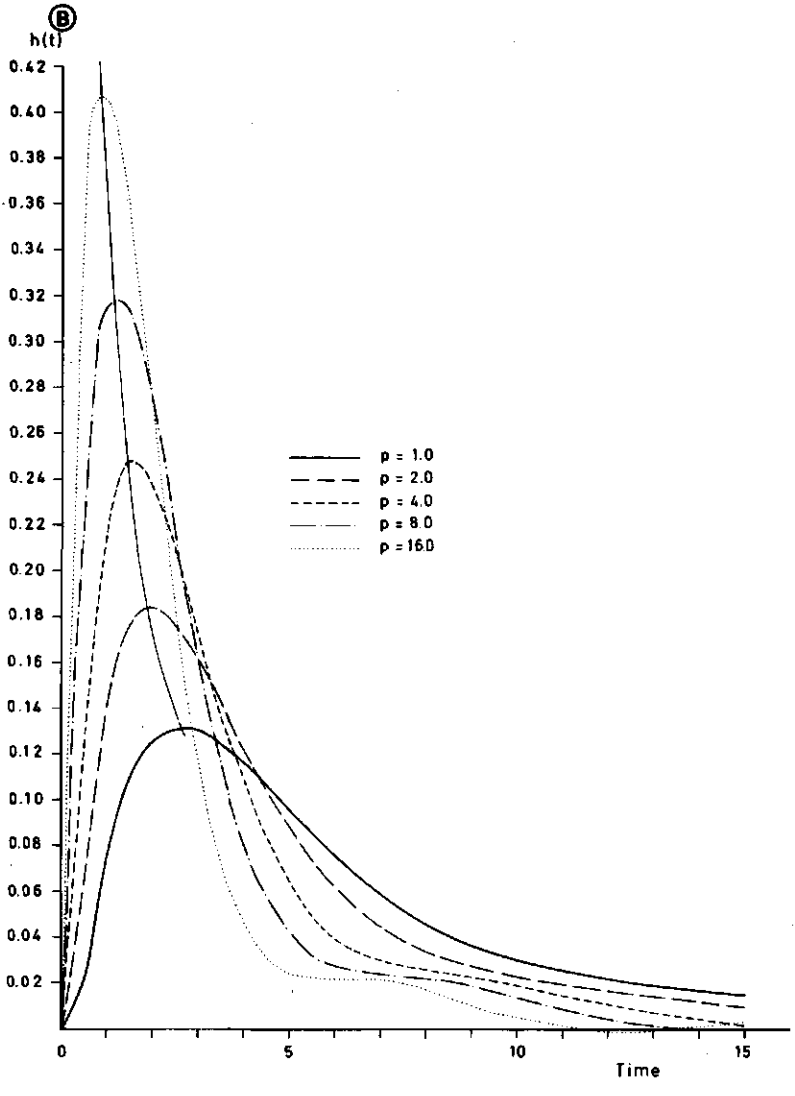

Fig. A3.4. Instantaneous unit hydrographs, $h(t)$, for constant inflows of variable magnitude. A. Duration T 16. B. Duration T 3.

Table A3.2. Influence of value of block-shaped inflows, p, on $h(t)$. For both T 3 and T 16 the time-scale factor $Z = \Delta t/2$; 20 Laguerre functions are used to approximate inflow and outflow.

T	p	Number of Laguerre functions for $h(t)$	$\int_0^\infty h(t)dt$	t_p	U_p	$t_p \cdot U_p$
3	1	7	1.01	2.6	0.132	0.34
	2	7	1.00	1.9	0.184	0.35
	4	10	1.00	1.4	0.248	0.35
	8	9	1.01	1.1	0.318	0.35
	16	12	1.04	0.85	0.405	0.34
16	1	5	1.01	2.5	0.176	0.44
	4	8	0.99	1.7	0.269	0.46
	8	9	1.00	1.4	0.332	0.47
	12	9	0.99	1.2	0.367	0.44
	16	8	1.02	1.2	0.380	0.46

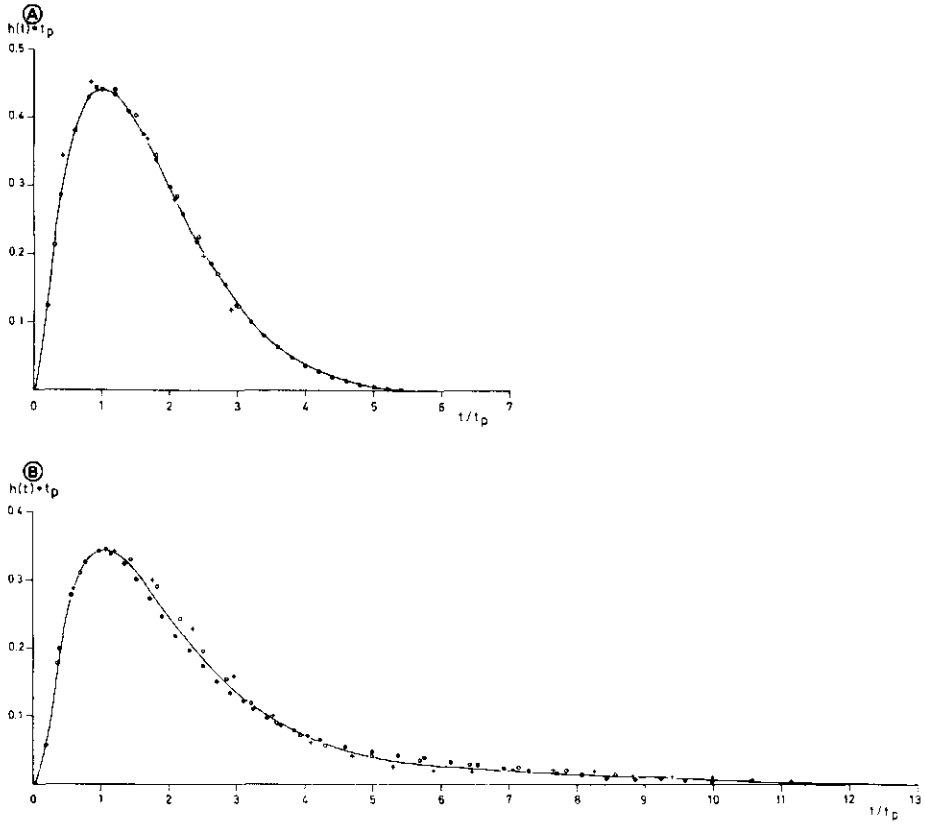

Fig. A3.5. Basic shape of IUH. A. Duration T 16. B. Duration T 3. ●●● from p = 1, ○○○ from p = 4, +++ from p = 16.

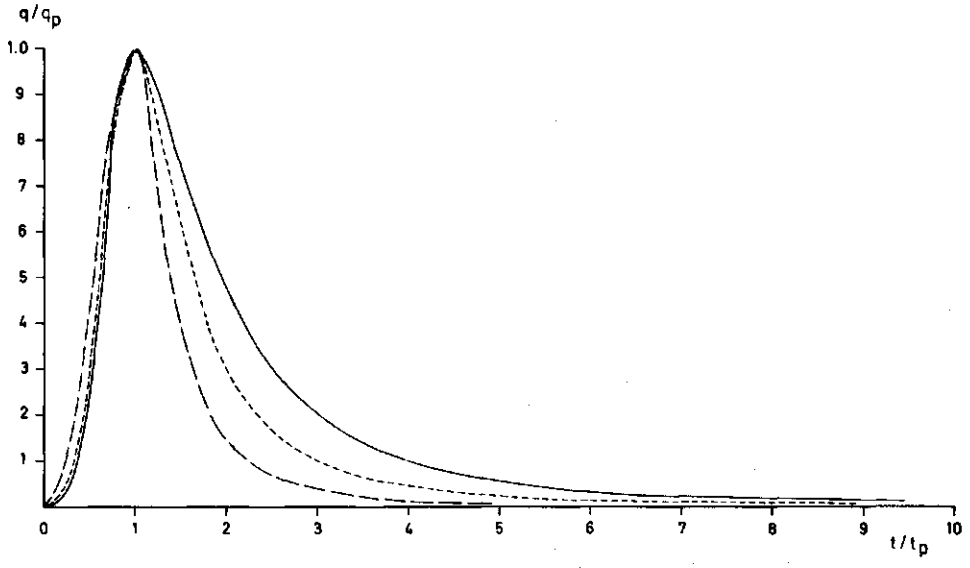

Fig. A3.6. Dimensionless outflow for $T = 3$ and $p = 1, 4$ and 16. — $p = 1$, ----- $p = 4$, – – – $p = 16$.

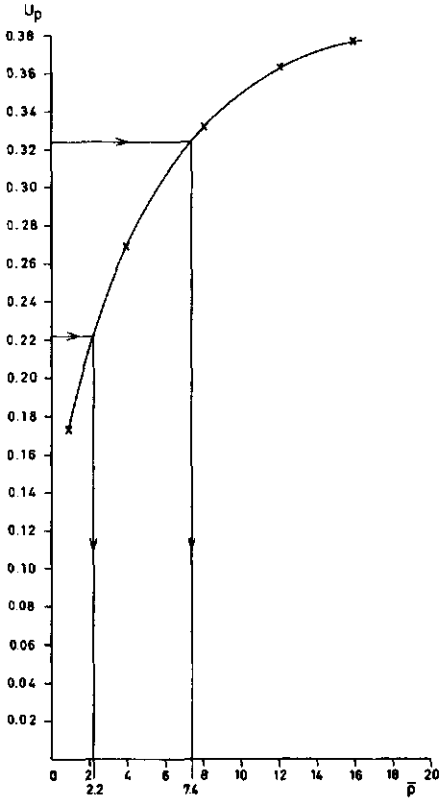

Fig. A3.7. Determination of boundary values for the average inflow $\bar{p}$.

of the inflow histogram is compared with the boundary values 2.2 and 7.4 as found in Figure A3.7.

For $\bar{p} < 2.2$, the IUH for $p = 1$,
$\bar{p}$ is 2.2-7.4 the IUH for $p = 4$,
$\bar{p} > 7.4$ the IUH for $p = 16$ was selected.

For a 'test storm' with an average input intensity $\bar{p}$ 4.0, the method is applied for six different 'extents of influence'. For the six simulations, the sum of squared differences between calculated and simulated outflow was determined. The result is given in Table A3.3, together with that of the linear simulation as obtained with the IUH for p 4. For the sum of squared differences as a function of the extent of influence, no single minimum was found. Hence no good criterion for the optimum length could be derived from the experiment. However the simulations with a length $\leqslant 5$ all give an improvement in the sum of squared differences compared to the linear simulation.

Figure A3.8 gives the simulation that uses an extent of influence for $\bar{p}$ of one time unit (so only the height of a bar of the histogram itself is used to select an IUH for that bar). It also gives the linear simulation.

Experiment with the outflow peak q_p as criterion

As in the previous experiment, the three IUH for T 16 and p 1, 4 and 16 are used. As the five IUH from Figure A3.4A were obtained with outflows of which the peak equalled the inflow, the boundary values of the peak of outflow q_p to select an IUH appropriate for a corresponding part of the histogram could be found as follows:

For $q_p < 2.5$: select the IUH for $p = 1$
q_p is 2.5-10.0 : select the IUH for $p = 4$
$q_p > 10.0$: select the IUH for $p = 16$.

As a first estimate of the four peaks of outflow, the peak values of the linear simulation were chosen. Quasilinear simulation showed that the first part of the histogram (time 0-5) was convolution-integrated with the IUH for p 16, whereas the rest of the histogram was convolution-integrated with the IUH for p 4 (Fig. A3.9).

Table A3.3. Effect of the length of the extent of influence on the outflow simulation.

Extent of influence	Sum of squared differences
1	14.3
2	23.7
3	23.7
4	23.2
5	14.5
6	50.3
Linear simulation with the IUH for p = 4.0	47.7

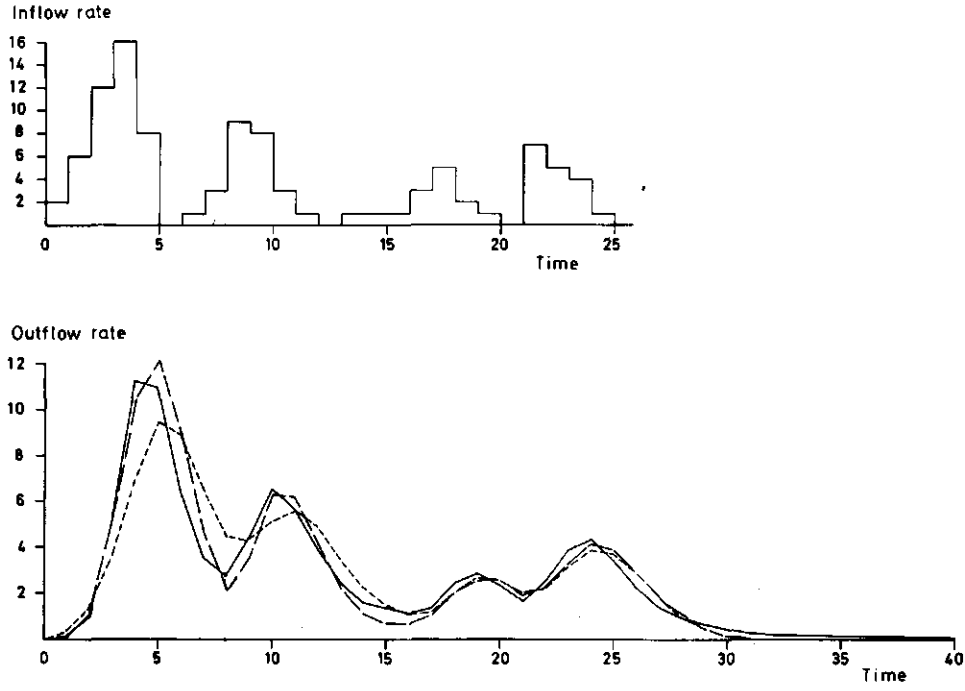

Fig. A3.8. Quasilinear simulation of outflow with the average inflow $\bar{p}$. Extent of influence for calculating $\bar{p}$. is 1 time unit. — calculated outflow, ----- linear simulation, – – – quasilinear simulation.

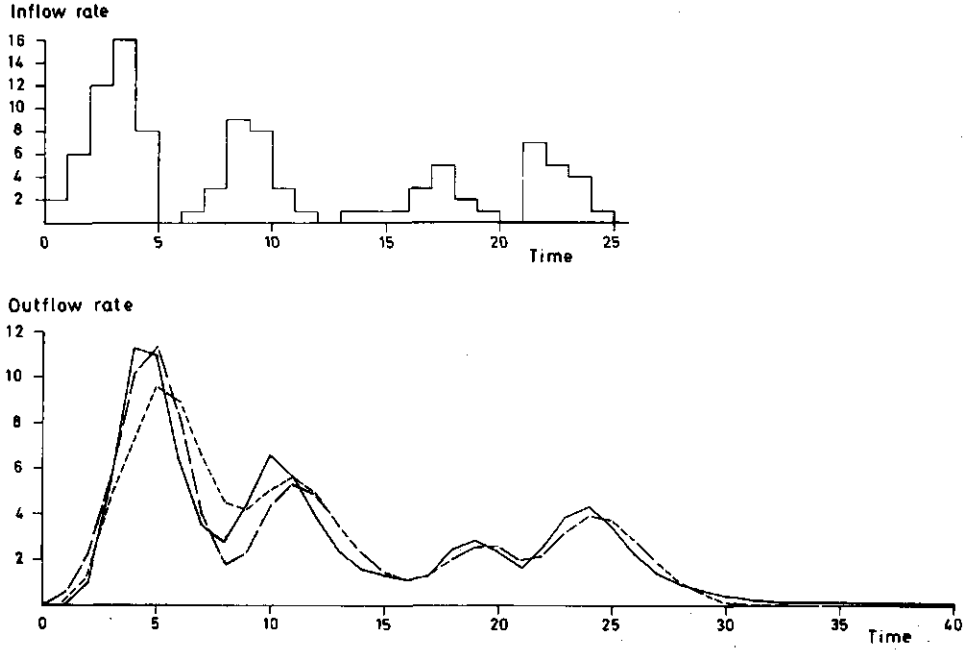

Fig. A3.9. Quasilinear simulation of outflow with the peak of outflow, q_p, as criterion for choosing one IUH out of three (T 16). — calculated outflow, ----- linear simulation – – – quasilinear simulation. Sum of squared differences: linear simulation 47.7, quasilinear simulation 22.2.

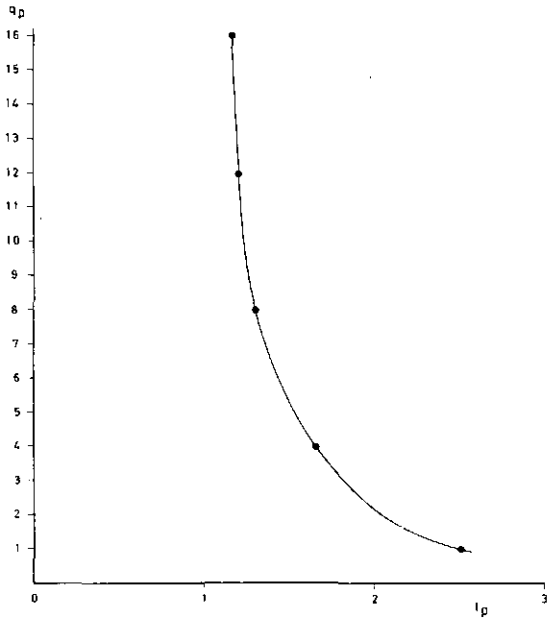

Fig. A3.10. Relation between the peak of outflow, q_p, and the time to peak of the IUH, t_p, for T 16.

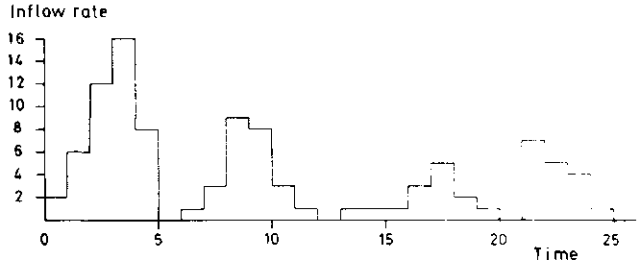

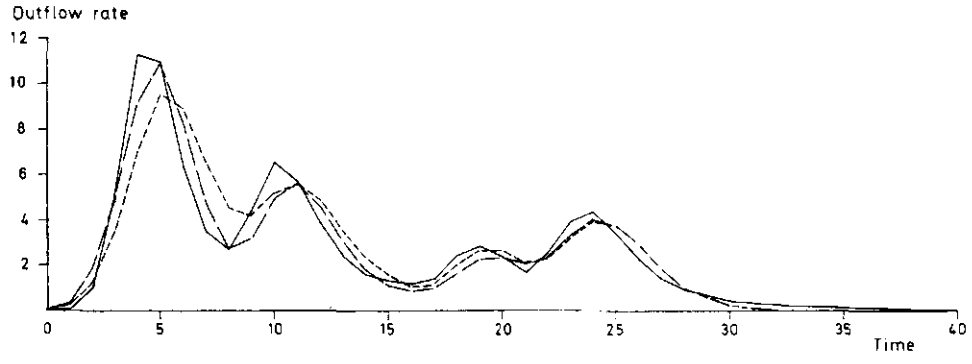

Fig. A3.11. Quasilinear simulation of outflow with the peak of outflow, q_p, as criterion, using the basic shape of IUH (T 16). — calculated outflow, ----- linear simulation, – – quasilinear simulation. Sum of squared differences: linear simulation 47.7, quasilinear simulation 19.1.

Comparison of the two quasilinear methods indicates that the method based on peak rates of run-off is more promising. For this method, the experiment is therefore repeated with the basic shape for T 16 from Figure A3.5A. To convert the basic shape in an IUH corresponding with a certain peak of outflow q_p, a relation was determined between the peak of outflow and the time to peak of the IUH t_p for the five IUH for T 16 (Fig. A3.10).

As initial values for the four peaks of outflow, the values from linear simulation were again taken. Next the corresponding t_p was obtained with Figure A3.10. For the four values of t_p, corresponding IUH was obtained from the basic shape of IUH. Next the outflow of the 'test storm' was simulated by convolution-integrating the four parts of the input histogram with their corresponding IUH and superposing the so obtained outflows (Fig. A3.11). One iteration of this procedure indicated no further change, so the outflow in Figure A3.11 is the final one. The simulated outflow appears to be slightly better than the simulation with three IUH (Fig. A3.9).

For the second of the two methods, the experiment was repeated with the other duration of inflow T 3. With the five IUH for T 3 (Fig. A3.4B), a relation between the peak of outflow q_p and the time to peak of the IUH t_p was determined (Fig. A3.12). A basic shape of IUH for T 3 was already determined (Fig. A3.5B). Again the outflow from the 'test storm' was simulated. For linear simulation, the basic shape of IUH was also used. To obtain t_p for this linear solution, it was decided to use the average of the four peaks of outflow of the 'test storm', $\overline{q_p}$. With Figure A3.12, a value for t_p was obtained. With t_p, the appropriate IUH could be derived from the basic shape of IUH.

Convolution-integrating the histogram of the 'test storm' with this IUH yielded a linear simulation. The quasilinear simulation, together with the linear simulation is given

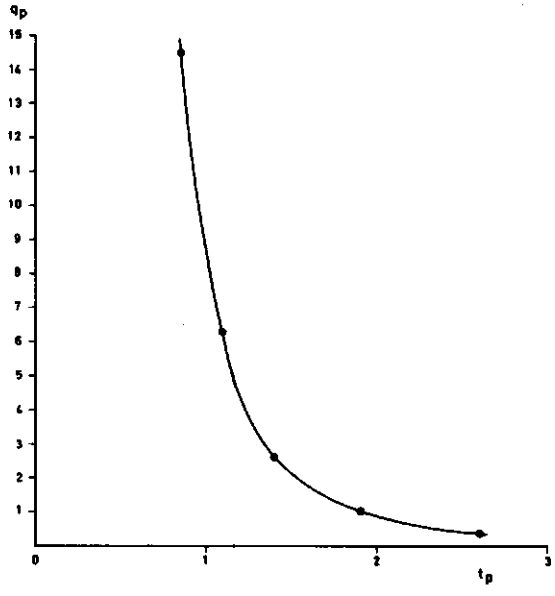

Fig. A3.12. Relation between the peak of outflow, q_p, and the time to peak of the IUH, t_p, for T 3.

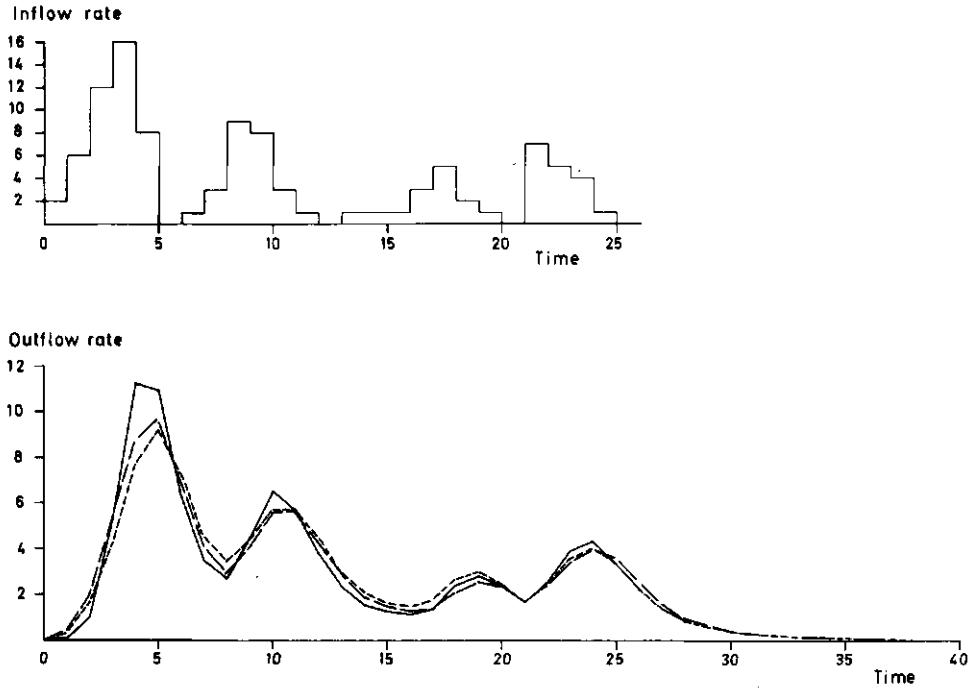

Fig. A3.13. Quasilinear simulation of outflow with the peak of outflow, q_p, as criterion, using the basic shape of IUH (T 3). — calculated outflow, ----- linear simulation, —·— quasilinear simulation. Sum of squared differences: linear simulation 20.8, quasilinear simulation 11.8.

in Figure A3.13. The difference in performance between the linear and the quasilinear solution is here not great. Both linear and quasilinear simulations are better than the corresponding simulations in Figure A3.11 for T 16.

Conclusions and remarks on the results of the experiments are given at the end of Chapter 4.